Coral Reefs
March 2024, Volume 43, Pages 415-428
https://doi.org/10.1007/s00338-024-02477-w
https://archimer.ifremer.fr/doc/00880/99223/

Mesophotic zone as refuge: acclimation and in-depth proteomic response of yellow gorgonians in the Mediterranean sea

Beauvieux Anaïs [8, *], Mérigot Bastien [8], Le Luyer Jeremy [2], Fromentin Jean-Marc [1], Couffin Nathan [3, 4], Brown Adrien [3, 4], Bianchimani Olivier [5], Hocdé Régis [8], Aurelle Didier [6], Ledoux Jean-Baptiste [7], Bertile Fabrice [3, 4], Schull Quentin [1]

[1] MARBEC, Univ Montpellier, Ifremer, IRD, CNRS, Sète, France
[2] Ifremer, IRD, Institut Louis-Malardé, Univ. Polynésie française, EIO, 98719, Taravao,Tahiti, Polynésie française, France
[3] Université de Strasbourg, CNRS, IPHC UMR 7178, 23 rue du Loess, 67037, Strasbourg Cedex 2, France
[4] Infrastructure Nationale de Protéomique ProFI, FR2048 CNRS CEA, Strasbourg 67087, France
[5] Septentrion Environnement, Marseille, France
[6] Aix Marseille Univ., Université de Toulon, CNRS, IRD, MIO, Marseille, France
[7] CIIMAR/CIMAR, Centro Interdisciplinar de Investigação Marinha e Ambiental, Universidade do Porto, Porto, Portugal
[8] MARBEC, Univ Montpellier, Ifremer, IRD, CNRS, Sète, France

* Corresponding author : Anaïs Beauvieux, email address : anais.beauvieux@gmail.com

Abstract :

The intensification of warming-induced mass-mortalities in invertebrate populations including in temperate regions is a critical global issue. Mesophotic zones (30–150 m depth) have been suggested as potential refuges from climate change for gorgonian populations, offering hope for reseeding damaged shallow populations. Using a proteomic approach, we investigated the responses and acclimatization ability of the yellow gorgonian Eunicella cavolini along an environmental gradient following reciprocal transplantations between shallow (20 m) and mesophotic (70 m) zones. Our findings indicate that yellow gorgonians from mesophotic waters exhibit a greater plasticity when transplanted to shallow waters, compared to shallow gorgonians transplanted to the mesophotic zone at 70 m. Transplanted colonies from mesophotic to shallow waters showed an increasing level of proteins involved in immune response but displayed no signs of necrosis or apoptosis, highlighting the acclimation potential of mesophotic populations. These results suggest that Eunicella cavolini populations may exhibit physiological plasticity in response to future climate change, allowing natural colonization from mesophotic populations. This analysis offers valuable insights into gorgonians' cellular and molecular responses to environmental changes.

Keywords : Deep sea refugia hypothesis, Eunicella cavolini, Global change, Molecular phenotype, Physiological plasticity, Reciprocal transplantations

Introduction

Marine communities are facing one of the worst periods in their recent history. Human activities, including pollution, habitat modification, and overfishing, have significantly impacted these ecosystems. The situation is further aggravated by climate change, which is causing rising seawater temperatures and extreme climatic events like marine heat waves (MHW, Oliver et al. 2018). MHWs globally impact marine ecosystems (Garrabou et al. 2009; Smith et al. 2023), harming various organisms (from corals to fishes) and habitats. The Mediterranean Sea is highly vulnerable to warming and MHWs (Garrabou et al. 2009; Aurelle et al. 2022). With its semi-enclosed temperate warm nature, it undergoes pronounced seasonal stratification and experiences elevated and fluctuating summer temperatures in shallow waters. In recent decades, MHW-associated mass mortality events have significantly impacted marine rocky benthic communities across extensive coastal regions, reaching depths of up to 30 m in the NW Mediterranean. Notable occurrences took place at the end of the summers of 1999, 2003, and 2022, spanning thousands of kilometres (Garrabou et al. 2009, 2022; Grenier, Marie et al. 2023).

Several gorgonian species, such as *Paramuricea clavata* and *Eunicella cavolini*, have been impacted by these mortality events (Garrabou et al. 2001, 2009; Linares et al. 2008; Estaque et al. 2023). Gorgonian species, as ecosystem engineers, play vital roles in benthic systems by serving as habitats, nurseries for fishes, and promoting high biodiversity (Enrichetti et al. 2019). Their decline or disappearance has severe consequences for the diversity and functioning of hard-bottom habitats (Enrichetti et al. 2019; Gómez-Gras et al. 2021). However, the impact of environmental stressors on these organisms is not spatially uniform, and certain areas may serve as temporary or long-term climate refuges, partially protected from warming disturbances (Glynn 1996; Bongaerts et al. 2010; Bramanti et al. 2023). Glynn (1996) proposed that mesophotic populations (30-150 m) could serve as climate refuges, with cooler and more stable conditions that are less impacted by thermal stress. This suggests the potential for reseeding shallower zones.

Experimental studies on Mediterranean octocorals have yielded mixed findings regarding thermotolerance levels. Non-symbiotic species like *Corallium rubrum* and *Eunicella cavolini*, with shallow populations (exposed to greater variability and potentially stressful conditions) exhibiting higher thermotolerance than mesophotic populations (up to 40-50 m depth; Haguenauer et al. 2013; Ledoux et al. 2015; Pivotto et al. 2015). Contrastingly, symbiotic white gorgonian *Eunicella singularis* showed stronger stress signals in shallow populations compared to mesophotic populations (15 m vs 35 m; Ferrier-Pagès et al. 2009), while both populations had similar necrosis threshold temperatures (Pey et al. 2013). Disentangling the respective contribution of plasticity and genetic

adaptive capacity in these gorgonian responses would require further investigation. Indeed, studies focusing on genetic structure between depths in Mediterranean octorallian revealed species-specific results. While, *Corallium rubrum* displayed strong patterns of genetic structuring along depth (Ledoux et al. 2010; Costantini et al. 2011), low genetic differentiation was observed between shallow and mesophotic populations of *Eunicella cavolini* (20 m vs 40 m, Pivotto et al. 2015). Displaying a low genetic structuring along depths and higher thermolerance, a wide bathymetric distribution from ca. 5 m to more than 100 m (Sini et al. 2015) and being a non-symbiotic gorgonian, *Eunicella cavolini* revealed itself as a great model for studying plasticity of mesophotic and shallow populations in a context of climate change.

Species impacted by climate change often display modifications in their physiology, distributions, and phenology (Hughes, 2000). Despite the large number of studies on monitoring mass mortality events (Garrabou et al. 2001, 2009, 2022; Estaque et al. 2023), the molecular and physiological mechanisms underlying this variety of thermotolerance remain poorly understood (but see Pratlong et al. 2015 for red coral). The physiological response to stress is indeed complex and many metabolic pathways and proteins are presumably involved in this process. Recent molecular technologies have extended the definition of the phenotype, as the composite of an organism's observable characteristics, to include measurable molecular characteristics, such as gene expression levels. This corresponds to the molecular phenotype (Ranz and Machado 2006). Transcriptional profiling is widely used to study the response of an organism to an extrinsic or intrinsic stressor, however, targeting only gene expression may be limiting. Indeed, many studies have shown a poor correlation between mRNA and protein levels (Abbott 1999; Mayfield et al. 2016). Proteomics appears as an appropriate approach to gain further insight into the molecular and cellular basis of stress response by directly measuring the abundance of proteins, i.e. the ultimate functional molecules.

We conducted a reciprocal transplant experiment to examine the molecular phenotypic plasticity of mesophotic and shallow gorgonian populations using proteomics. Colonies of the non-symbiotic yellow gorgonians *Eunicella cavolini* were reciprocally transplanted between shallow (20 m depth, experiencing increasing water temperatures during summer) and mesophotic habitats (70 m depth, below the thermocline where temperatures remain stable throughout the year (Bensoussan et al. 2010). Using a shotgun proteomic approach this study investigated (1) whether colonies from distinct shallow and mesophotic environments exhibit distinct molecular phenotypes (Ranz & Machado 2006)? If local adaptation or acclimation occurs, protein expression profiles of shallow *vs* mesophotic colonies are expected to diverge; (2) do colonies from these two contrasted environments show different acclimatization capacity? We investigated the molecular phenotype of transplanted colonies compared to colonies

of their origin or destination depths. High plasticity will be reflected by an important shift in molecular phenotype between transplants and their controls; and (3) what are the underlying molecular processes involved in local adaptation or acclimation? We investigated the molecular pathways differentially expressed between transplants and controls, and discussed their implication regarding climate change (Reusch 2014) and the deep-sea refuge hypothesis (Glynn 1996).

Materials and Methods

Contrasted environmental conditions along depth and reciprocal transplant experiment

From late autumn to winter (December–March), seawater temperatures, in the Marseille area, northern Mediterranean Sea, slowly decline, reaching a minimum in March of about 13 °C along the entire water column, before rising slightly until the formation of the thermocline (Figure 1, Bensoussan et al. 2010). In summer, above this thermocline (~20-30 m depth), strong temperature oscillations may reach 12 °C (Pivotto et al. 2015), and very low nutrient concentrations have been described in open sea (Pasqueron de Fommervault et al. 2015). On the other hand, mesophotic waters (below the thermocline, 30 m-150 m) display more stable thermal regime (Bensoussan et al. 2010), with potentially higher nutrient concentration but higher-pressure conditions (e.g. 8 bars at 70 m).

A reciprocal transplant experiment was performed from June to November 2021 (spanning over the summer and the beginning of autumn period during which MHW mortality events usually occur) with specimens from two yellow gorgonian populations inhabiting the rocky coast around Marseilles (NW Mediterranean Sea). The water temperature was relatively homogeneous along depths at the moment of the transplantation, and for about two weeks at sampling (Figure 1). The populations were sampled from shallow and mesophotic waters around the Impérial du Large (43°10’11.5”N 5°23’40.0”E): 20 m (shallow population) and 70 m depth (mesophotic population). Considering the limited dispersal abilities of larval stages in Mediterranean octocorals (Martínez-Quintana et al. 2015; Masmoudi et al. 2016), colonies were sample at a distance of 20-30 m from each other in order to encompass a wide range of geographic and genetic diversity at each depth. The experiment included four different treatments: two control colonies transplanted at their native depth (Control Shallow (C_{20}) and Control Mesophotic (C_{70})) and two transplants, transplanted at either 20 m or 70 m (Mesophotic to Shallow ($T_{70\rightarrow 20}$) and Shallow to Mesophotic ($T_{20\rightarrow 70}$); Figure 2). A single colony (identical genotype) provided one fragment control (C) and one fragment transplants (T).

The apical tips (8 cm) of four fragments (two replicates) per colony were randomly sampled via closed-circuit rebreather and fixed underwater on experimental plates (see ESM1). Overall, the experiment involved sixteen

colonies from two populations (eight shallow and eight mesophotic), shared among eight plates (two plates per treatment). Sampling occurred mid-November (five months post-transplantation). Tissues were removed, frozen immediately in liquid nitrogen, and stored at −80 °C until further analysis.

Quantitative shotgun-proteomics analysis

Procedures for sample preparation, nanoLC-MS/MS analysis, and mass spectrometry data analysis are detailed in ESM2. Samples were analyzed on a nanoUPLC-system (nano-Acquity, Waters, Milford, MA, USA) coupled to a quadrupole-Orbitrap hybrid mass spectrometer (Q-Exactive HF-X, Thermo Scientific, San Jose, CA, USA). Two samples were excluded from the proteomic analysis due to unsatisfactory protein extraction. Two additional individuals (one $T_{70\rightarrow 20}$ and one $T_{20\rightarrow 70}$) were removed because of a high number of missing values. Altogether, 28 samples were analysed.

Protein functional annotation

We used ORSON https://gitlab.ifremer.fr/bioinfo/workflows/orson for sequence similarity search (PLAST, Noël et al. 2021), functional prediction using InterProScan (Quevillon et al. 2005) and Blast2GO to extract GO-terms (Conesa et al. 2005).

Statistical Analysis

Data were filtered to retain proteins present in at least 70% of individuals in each treatment, resulting in a set of 2610 expressed proteins. 1620 missing values (2% of the dataset) were imputed using the random forest method. This method showed strong performance and proved to be the most suitable approach for label-free proteomic studies when the missingness mechanism is not fully understood (Jin et al. 2021). Analyses were performed in R v.4.1.1 (R Core Team 2021).

Molecular phenotypic plasticity

To investigate the molecular phenotype of the control groups (C_{20} and C_{70}), a discriminant analysis of principal components (DAPC, Jombart et al. 2010) from the 'adegenet' package was performed on the scaled protein intensities matrix. This analysis retained the first six principal components (PCs) that accounted for 70% of the total variance. The first discriminant function (LD1) served as a measure of molecular phenotype divergence. To quantify plasticity upon transplantation, we projected both transplanted colonies within the same multivariate plan and compared both transplanted treatments to their respective controls. The magnitude of these shifts in mesophotic and shallow gorgonians is proportional to the lengths of the blue and yellow arrows in Figure 2. These effect sizes were inferred using Markov chain Monte Carlo linear mixed models, with individual genotype

specified as random effect and analysing 1,800 samples of parameter estimates to derive P-values for population-specific differences ('MCMCglmm' package).

Co-expression network and functional enrichment analyses

Gene co-expression network

Using a Weighted Gene Coexpression Network Analysis (WGCNA) (Langfelder and Horvath 2008) on log-transformed proteins abundances matrices, proteins were grouped into modules. The soft threshold for network construction was chosen to ensure that the constructed network closely fit a true biological network state (beta = 6; $R^2 = 0.91$). The default setting of a minimum of 30 proteins per module ensured sufficient protein representation for subsequent functional enrichment analysis. Proteins that did not fall within any modules, indicating low co-expression, were grouped into a separate grey module. Then, we investigated whether module's eigengenes correlate with treatment conditions (i.e Controls: C_{20} *vs* C_{70}; Transplants against native depths: $T_{70\rightarrow20}$ *vs* C_{70}; $T_{20\rightarrow70}$ *vs* C_{20} and Transplants against destination depth: $T_{70\rightarrow20}$ *vs* C_{20}; $T_{20\rightarrow70}$ *vs* C_{70}).

Functional enrichment

Functional enrichment analysis was performed following two complementary methods: 1) for each module that correlated with a treatment, we investigated whether the proteins within belonged to specific molecular pathways (Gene Ontology (GO) terms), and 2) independently of modules we assessed whether proteins displaying high level of GS association with a treatment belonged to specific molecular pathways (GO terms) (Langfelder and Horvath 2008). In both approaches, the "background" for the enrichment analysis was the functionally annotated proteome of *Eunicella cavolini*, which consisted of 20,420 proteins. This subset represents around 40% of the 51,038 predicted proteins (including isoforms and potential protein “fragment”) for this species (see ESM2 for further details about the predicted proteome). This comprehensive background ensures a robust assessment of functional enrichment relative to the entire proteome and is particularly noteworthy given that *E. cavolini* is a non-model species (Heck and Neely 2020). GO term delta rank represents the difference between the mean ranks of the proteins belonging to the specific GO term and the mean ranks of all proteins that the considered GO term do not include. Positive delta ranks indicate an increased tendency, while negative delta ranks indicate a decrease tendency of the GO term considered. It has been tested using i) Fisher's exact tests on binary response for membership to the module and ii) using two-tailed Mann-Whitney U test when considering GS. We used the package ‘*GO_MWU’* particularly suitable for non-model organisms (https://github.com/z0on/GO_MWU) (Dixon et al., 2015). Enriched GO terms are displayed in a dendrogram plot. Distances between GO terms reflect the

number of shared proteins. Global network visualization was done using Cytoscape V3.9.1 (Shannon et al. 2003) in ClueGO v2.5.9 (Bindea et al. 2009).

Functional Comparison between transplants

In order to compare the functional response similarity between treatments, their respective GO term delta ranks were plotted against each other. The strength of the relationship indicates the similarity of enrichment. It is important to note that these plots do not represent a formal statistical test since the data points (gene ontology categories) are not independent, as they often include overlapping sets of proteins. Nevertheless, they provide insights into functional similarity or dissimilarity in enrichments.

Results

At the end of the experiment, no necrosis nor mortality were observed in any of the four treatments (Control Shallow, Control Mesophotic, Mesophotic to Shallow, and Shallow to Mesophotic).

Transplantation reveals plastic protein expression

Molecular phenotypes between control mesophotic and control shallow gorgonians were well discriminated (low overlap between solid distributions, Figure 3) by the first eigenvector LD1 explaining 43% of the total variance. The molecular phenotypic shift of the two transplanted treatments were assessed by projecting their respective molecular phenotype within the same multivariate plan (light distributions, Figure 3). The magnitude of this shift represents a quantitative measure of protein abundance plasticity. Gorgonians transplanted from mesophotic to shallow habitats exhibited a significantly larger molecular phenotype shift than shallow gorgonians transplanted to mesophotic habitats ($P_{MCMC} = 0.04$, blue arrow). The former resulted in a nearly perfect match with the control Shallow molecular phenotype (light blue, Figure 3), while the latter mostly remained in between the two controls (light yellow, Figure 3).

Weighted Gene Co-expression Network Analyses

To delve into the underlying molecular mechanisms of *Eunicella cavolini'* plasticity, we performed a weighted gene co-expression network analysis (WGCNA). The analysis assigned all 2,610 log-transformed protein abundances to ten co-expression modules of 31 to 732 proteins (designated by colours, Figure 4). Eight module eigengenes displayed significant and strong correlations with treatments (Figure 4).

- Mesophotic vs Shallow

The comparison between the two control groups (C_{20} *vs* C_{70}) correlated with two modules (green and purple) that did not show any functional enrichment.

- Transplant *vs* Origin

Four modules (magenta, pink, turquoise and purple) correlated with the comparison $T_{70\rightarrow20}$ *vs* C_{70}. However, Gene Ontology (GO) enrichment analysis of proteins in these modules revealed no enriched GO terms.

The opposite transplant $T_{20\rightarrow70}$ *vs* C_{20} also showed significant correlation with four modules (green, purple, brown and blue). Among these modules, only the brown module displayed a significant GO enrichment. It included enrichment of eight GO terms related to metabolism, notably lipid metabolism and catabolism (*e.g. cellular lipid metabolic process* (GO:0044255), *long-chain fatty acid metabolic process* (GO:0001676) and *regulation of cellular catabolic process* (GO:0031331), Figure 5a), as well as cell organization (e.g. *regulation of cell-substrate junction organization* (GO:0150116), *regulation of cell-matrix organization* (GO:0001952) and *negative regulation of smooth muscle cell proliferation* (GO:0048662), Figure 5a). Within these eight enriched GO categories, six were under-represented in transplanted colonies compared to their control (z-score<0, Figure 5b), while two displayed little to no change (equivalent number of proteins with increased and decreased abundance, white rectangle, Figure 5b).

- Transplant vs Destination

$T_{20\rightarrow70}$ *vs* C_{70} displayed a significant correlation with the brown module described above. The same response was observed with the $T_{20\rightarrow70}$ *vs* C_{20} comparison displaying a general under-representation of the eight enriched GO categories in the transplanted colonies (ESM5). Finally, $T_{70\rightarrow20}$ *vs* C_{20} revealed positive correlation with three modules (turquoise, blue and red) without any significant functional enrichment.

Enrichment with gene significance

GO enrichment analysis based on the Gene Significance of each protein (correlation with a specific treatment) enabled the discovery of pathways that were significantly enriched, regardless of the module to which they were assigned. These results are displayed in Figure 6.

- Shallow *vs* Mesophotic

The comparison of the two control treatments (C_{20} *vs* C_{70}) exhibited a significant enrichment in seven GO, mainly related to metabolism and cell structure (*cell part morphogenesis* (GO:0032990), ESM6, Figure 6). Notably, four out of these seven GO over-represented in C_{20}, were similarly found in the comparison between $T_{70\rightarrow20}$ and their controls C_{70} (ESM6).

- Transplant vs Origin

$T_{70\rightarrow20}$ *vs* C_{70} rank-based functional enrichment analyses based on Gene significance, highlighted an enrichment in fourteen GO categories, mainly involved in metabolic pathways (e.g. *cellular amide metabolic process* (GO:0043603), *carbohydrate metabolic process* (GO:0005975)) and immune response (e.g. *innate immune response* (GO:0045087), *immune system process* (GO:0002376)) (Figure 6 & 7a). Proteins involved in immune pathways displayed a general decreasing abundance (z-score<0) while biosynthetic and metabolic GO terms were over-represented (z-score>0) except "carbohydrate metabolic process" which was under-represented in $T_{70\rightarrow20}$ (Figure 7c). By opposition, enrichment analysis for $T_{20\rightarrow70}$ *vs* C_{20} displayed four of the same metabolic and biosynthetic GO terms differentially represented although under-represented (Figure 7b & d).

- Transplant vs Destination

While comparison between $T_{70\rightarrow20}$ and C_{20} colonies revealed no functional enrichment, the comparison $T_{20\rightarrow70}$ *vs* C_{70} exhibited twenty one enriched GO categories mainly involving cell organization and adhesion pathways (e.g. *cell adhesion mediated by integrin* (GO:0033627), cellular developmental process (GO:0048869), *external encapsulating structure organization* (GO:0045229), ESM7, Figure 6). All enriched categories were under-represented in $T_{70\rightarrow20}$ compared to C_{20} (ESM7).

Comparison of the delta-rank values between $T_{70\rightarrow20}$ *vs* C_{70} and $T_{20\rightarrow70}$ *vs* C_{20} revealed a low but significant negative correlation (cor = -0.20, $p<0.01$), highlighting similarities in the processes involved, displaying opposite responses to transplantations.

Discussion

Climate change affects a number of physiological and metabolic changes in cnidarians, as already well-studied in hexacorals (Brener-Raffall et al. 2019; Dixon et al. 2020). Our study is the first to compare the proteomic patterns in temperate octocorals inhabiting contrasting mesophotic and shallow zones. The choice of a cnidarian that does not host algal symbionts (*Symbiodiniaceae*) allowed us to overcome the effect of algal symbionts on stress

response and on adaptation/acclimation to local environment. After transplantation of *E. cavolini* colonies to different depths (i.e. Mesophotic to Shallow compared to Control Mesophotic and Shallow to Mesophotic compared to Control Shallow), we detected physiological responses that involved similar metabolic pathways and specific biological processes depending on the depths of origin or transplantation (albeit they were not similarly regulated). We also highlighted processes that were specifically affected after transplantation in shallow water.

Differential phenotype between depths

Relying on "Gene Significance" GS, we evidenced functional enrichment in metabolism pathways between colonies from different depths in basal condition (control treatments: C_{20} *vs* C_{70}). Higher temperatures in shallow waters compared to 70 m (Figure 1) could lead to increase energy metabolism in shallow colonies compared to colonies that stayed at 70m. These results highlight that environmental conditions at each depth act on protein regulation. Such modification may reflect local genetic adaptation or acclimation leading to different molecular phenotype. Considering protein regulation as a molecular phenotype, we therefore demonstrated that phenotypes are significantly different in individuals inhabiting different depths. This may provide insights into the underlying molecular processes contributing to the observed variations in the levels of thermotolerance (survival/necrosis) within the same area for *E. cavolini* up to a depth of 40 m (20 m vs 40 m; Pivotto et al., 2015).

On the whole-proteome level, are mesophotic colonies more plastic than their shallow counterparts?

At the whole-proteome level, we observed a substantial plastic convergence of mesophotic colonies when transplanted in shallow waters (Figure 3). Interestingly, our analysis suggests that gorgonians from mesophotic waters may exhibit a more plastic response to being transplanted into shallow waters, compared to native shallow gorgonians transplanted at 70 m. Although this result should be taken with caution in regard to the large number of protein considered and the rather low number of individuals, it is consistent with functional enrichment (KOG and GO). Altogether it shows that transplants "Mesophotic to Shallow" presented the same molecular phenotype as colonies staying at 20 m (no GO categories and nor KOG were significantly enriched ESM3 and ESM4), whereas transplants "Shallow to Mesophotic" showed an intermediate phenotype (Figure 3). Indeed, shallow colonies placed at 70m fall short of displaying the protein expression of control mesophotic colonies. This difference may be attributed either to a lower phenotypic plasticity or to a lower constraining environmental change. Building on this idea, an additional explanation would be that the five-months duration of our study was not sufficient for these colonies to establish a molecular phenotype similar to control individuals at 70 m. Alternatively, individuals at shallow depths where temperature fluctuations are of higher magnitude during summer (Figure 1) may be under stronger environmental constraints and therefore display local adaptation. As a

consequence, being well adapted to shallow water could constrain their phenotypic plasticity as we observed when transplanted at 70 m. Enrichment analysis of the transplantation to mesophotic waters revealed a general decrease of proteins abundance involved in cell structure and cytoskeleton (compared to control mesophotic treatment). Manual curation of the *E. cavolini* proteome revealed biomineralization "tool-kit" proteins (Drake et al. 2013), including calcium-binding proteins and skeletal organic matrix proteins (i.e. myosin, tubulin, actin etc.). Similarly, Tambutté et al. (2015) suggested that corals may increase levels of skeleton organic matrix proteins to promote calcification under less favourable calcifying conditions (such as higher temperature and lower pH) as it is partially the case in shallower water in the Mediterranean sea. This could explain the decreasing level of proteins involved in calcification for colonies transplanted to a more stable habitat at 70 m. While the identification of cytoskeleton proteins may be influenced by their abundance in eukaryotic cells, our finding aligns with previous works highlighting that cytoskeleton is emerging as a common target of stresses from multiple origin (Tomanek 2014). It can also hypothesize that this under-representation is a physiological acclimation of native shallow colonies confronted to higher pressure condition at 70 m. Reduced abundance of proteins involved in calcification could suggest a decrease in growth rate of these transplanted colonies. Assessing ultimate fitness would help disentangling the mechanism involved and their long-term consequences which call for further research.

Our results lend additional support to an emerging insight that protein expression plasticity may play a substantial role in migrants' adaptation to novel environments. Kenkel & Matz (2017) subjected mustard hill coral (*Porites astreoides*) to a reciprocal transplant experiment across a temperature gradient, and likewise found transcriptomic convergence of migrants towards residents. A large body of existing studies suggest that increased plasticity occur in temporally or spatially heterogeneous habitats (Baythavong 2011). Our result present an intriguing puzzle as we observe greater proteomic plasticity in gorgonians from mesophotic population, despite their seemingly more stable habitat. Mesophotic environment still remain poorly studies especially in coastal areas and its local environment may vary in other ways (biotic and abiotic; food, sediment…) potentially affecting molecular phenotypes. Altogether this definitely urges for further investigation of the mesophotic ecosystems (Bramanti et al. 2023).

Transplantation into non-native habitats reveals static and plastic protein expression

The set of pathways enriched in both transplanted colonies (Mesophotic to Shallow and Shallow to Mesophotic) suggests a common response to transplantation with opposite regulation patterns. While energy metabolism pathways were all over-represented in the colonies Mesophotic to Shallow (vs Control Mesophotic), those same functions were under-represented in the opposite treatment (Shallow to Mesophotic vs Control Shallow). As

previously suggested, elevated temperatures in shallow waters is expected to upregulate energy metabolism. Notably, this increase did not encompass carbohydrate metabolism as it was under-represented. Accordingly, Tignat-Perrier et al. (2022) described in the same species and a close relative (the red gorgonian *Paramuricea clavata*) a significant reduction of carbohydrates reserves at the end of a seven week of experimental thermal stress (-58% in *P. clavata* and -45% in *E. cavolini*). This under-representation may be amplified by the low nutrient concentrations in shallow water compared to mesophotic waters during summer (Pasqueron de Fommervault et al. 2015). While a high metabolism can lead to elevated levels of Reactive Oxygen Species (ROS) and cellular damage (Lesser 2006), the response to oxidative stress and the apoptotic process remained unaffected in our study unlike previous results reported for *S. pistillata* being transplanted from 60 to 20 m (Malik et al. 2021). Simultaneously, we observed a decrease in the abundance of proteins associated with the calcification process in colonies transplanted to shallow waters in comparison to colonies from the control Mesophotic treatment. Accordingly, a downregulation of genes involved in calcification in colonies from another octocoral *Pinnigorgia flava* exposed to heat stress was previously observed (Vargas et al. 2022).

Colonies transplanted at 70 m displayed an opposite response with a global under-representation in all enriched metabolism pathways. Simultaneously, shallow to mesophotic colonies revealed decreasing level of proteins related to lipid metabolism and transport (compared to their control) in accordance to reduced energy metabolism. Previous studies quantifying respiration responses have highlighted that mesophotic zooxanthellate corals exhibit depressed metabolic rates compared to their shallower conspecifics (Lesser et al. 2010; Cooper et al. 2011). These findings align with our observation in non-symbiotic octocoral and call for further research to characterise their local abiotic and biotic environment. Characterising local stressor and positive drivers of growth and maintenance will aid in understanding underlying mechanisms and ultimate fitness consequences of the local environment on the resilience of this sessile species to climate change.

One of the main results of our experiment was a decreasing level of proteins involved in immune response in colonies transplanted from mesophotic to shallow zones. Environmental stressors have already been linked to immunosuppression in other invertebrates such as oysters (Raftos et al. 2014) and patterns of immunosuppression in corals have been observed in zooxanthellae hexacorals during and after bleaching (Pinzón et al. 2015). These immunosuppressive response has been suggested to result from the increase in new diseases and disease prevalence after bleaching (Raftos et al. 2014) and may be induced by increasing pathogens prevalence in close related species during MHW (see Prioux et al. 2023 for an example in *Paramuricea clavata)*. However, the absence of necrosis and of typical molecular stress pathways in this present studies (*e.g.* reduction of ribosomal representation,

increased levels of heat shock proteins and antioxidants (Desalvo et al. 2008, 2010; Császár et al. 2009)) leaves the door opens to alternative hypotheses. The absence of common molecular response to stress might be attributed to the timing of sample collection, which occurred considerably after the onset of potential stress responses. Indeed, in our study the proteomic response was assessed five months after reciprocal transplantation and at least two weeks after the water temperature dropped below 21 °C (Figure 1). This timeframe contrasts with other studies that have examined physiological responses within few days of exposure to stressful conditions. Secondly, the immune system that undergoes suppression may allow to reallocate resources to other metabolic demands (Deerenberg et al. 1997; Demas et al. 1997) such as cytoskeleton modulation, as evidenced by an increasing energy metabolism in this study. This hypothesis posits trade-offs between immune system and other primary functions, suggesting that significant energy savings can be achieved by suppressing the immune system. However, further investigation is needed, particularly focusing on the associate microbiome and its dynamic after transplantation. Alternatively, immunosuppression might occur as the organism's attempt to mitigate autoimmune damage in times of stress (Råberg et al. 1998). In our case, transplantation led to cytoskeleton modifications, potentially altering the self-antigen repertoire and triggering an immune response akin to that observed in tissues damaged by disease. As previously suggested, optimal functioning might involve suppressing immune responses to avoid immunopathology (Bagby et al. 1994). Monitoring immune function and cytoskeleton on a shorter time scale (e.g. monthly) during the summer would enhance our understanding of the trade-offs and progressive acclimation occurring in this species.

Implications for gorgonian acclimation to climate change

The molecular shift in mesophotic colonies transplanted to shallow waters (i.e., overall increasing metabolism) suggests capacity for acclimation. This finding demonstrates that the *E. cavolini* populations examined in this study display physiological plasticity in response to environmental stress, at least over the time scale of our study (i.e. five months). Nevertheless, the metabolic remodelling of *E. cavolini* in shallow waters involved an increased abundance of energy metabolism-related proteins. This aligns with the hypothesis that such acclimation is energetically demanding, raising questions about its effectiveness in coping with thermal stress, such as a marine heatwave. A rigorous evaluation of this hypothesis would require direct measurements of respiration rates, energy reserves and ultimate impact on fitness, underscoring the need for further research in this area.

Furthermore, despite immunosuppression, the colonies displayed no signs of necrosis or apoptosis, emphasizing the acclimation capacity of this species. Notably, heat-shock protein homologues (five HSP70, one HSP60, one HSP90 and two HSP10) were detected at both depths, but their abundance did not show significant differences.

While this contrasts with short term experimental stress on the Mediterranean red coral (*Coralium rubrum*) where HSPs were involved in stress response (Haguenauer et al. 2013), it also suggests that several months of exposition may be sufficient to recover HSP levels to baseline. Alternatively, these results could be attributed to the absence of massive thermal anomalies in the Marseille area during that specific year (Figure 1). Seawater temperature did not reach 24 °C at 20m that summer (Figure 1b), the critical temperature for two other Mediterranean gorgonian species being 25°C (*P.clavata* and *C.rubrum*, Ledoux et al. 2015; Garrabou et al. 2022). Additionally, *E. cavolini* did not exhibit necrosis when experimentally reared at 23 °C (~100% of necrosis at 27.5 °C for 36 days; Pivotto et al. 2015). Nevertheless, further research on the physiological signature of organisms presenting necrosis is needed to identify the underlying cellular processes involved.

Overall, our findings suggest a significant capacity of *E. cavolini* to cope with potential stressful conditions, aligning with previous reports (Previati et al. 2010; Tignat-Perrier et al. 2022). However, a recent episode of mass mortality during the summer of 2022 in NW Mediterranean Sea affected gorgonians, resulting in mortality rates of up to 80% between 0 and 30m of depth for *P.clavata* and to a lower extent for *E.cavolini (10-30%)* (Estaque et al. 2023). Ongoing proteomic analysis of individual identified as “resistant” vs. “vulnerable” in this region following this mass mortality event will provide insights into the molecular phenotype of necrotic individuals and the potential proteins involved in the differential responses of colonies and populations to thermal stress.

There is currently limited information on genetic connectivity between mesophotic and shallow gorgonian populations (but see Ledoux et al. 2010, Costantini et al. 2011, Haguenauer et al. 2013 for *C.rubrum*), representing a critical gap in understanding the role of mesophotic population in reef resilience. Nevertheless, given the escalating pressures on coral reefs, particularly at shallow depths (<30–40 m) (Bak et al. 2005; Bramanti et al. 2023), the findings of this study suggest the absence of physiological barrier to recolonization (but see Pivotto et al. 2015 for an experiment on thermotolerance). This reinforces the crucial role of mesophotic ecosystems as a potential source of recruits for their affected shallow counterparts. While our study clearly identified different response patterns between shallow and mesophotic populations, it is important to note that it focuses on a limited geographic area of the Mediterranean Sea. Therefore, there is a need to extend such approaches at a large geographic scale to validate our observations.

Conclusion

This pioneering study compares proteomic patterns of a temperate octocoral across individuals from diverse environmental conditions. By extending such approaches to an octocoral in a field where hexacorals are predominantly studied, it sheds lights on the potential acclimation of cnidarians to climate change. The observed expression patterns in mesophotic colonies transplanted to shallow waters indicate acclimation and highlight the molecular plasticity of *E. cavolini* populations in responses to environmental challenges. Importantly, this study suggests the absence of physiological barrier hindering natural recolonization from mesophotic colonies. It underscores the significance of mesophotic areas and emphasizes the need for further scientific investigation and careful consideration of these zones in the management plans of protected and exploited areas.

Acknowledgement

We gratefully acknowledge the support and cooperation of the Parc National des Calanques, Marseille, and Septentrion Environnement for their logistical assistance in the field. This work is part of the DEEP EVO and DEEP HEART projects funded by the Sea and Coast Key Initiative of Montpellier University of Excellence (KIM) and the Laboratory of Excellence Mediterranean Center for the Environment and Biodiversity (Labex CeMEB), respectively. ABe. acknowledges a PhD grant from the University of Montpellier–GAIA doctoral school. We also acknowledge the support provided by strategic funding from FCT–Fundação para a Ciência-e-a-Tecnologia through grants UIDB/04423/2020, UIDP/04423/2020, and 2021.00855.CEECIND. We express our gratitude to all those who contributed their sea water temperature data in T-mednet, with special thanks to Dorian Guillemain and Nathaniel Bensoussan. DA. is supported by the European FEDER Fund, project 1166-39417 and by Excellence Initiative of Aix-Marseille University-A*MIDEX, a French “Investissements d’Avenir” programme.

References

Abbott A (1999) A post-genomic challenge : learning to read patterns of protein synthesis. Nature 402:715–720

Aurelle D, Thomas S, Albert C, Bally M, Bondeau A, Boudouresque C, Cahill AE, Carlotti F, Chenuil A, Cramer W, Davi H, De Jode A, Ereskovsky A, Farnet A, Fernandez C, Gauquelin T, Mirleau P, Monnet A, Prévosto B, Rossi V, Sartoretto S, Van Wambeke F, Fady B (2022) Biodiversity, climate change, and adaptation in the Mediterranean. Ecosphere 13:1–23

Bagby GJ, Sawaya DE, Crouch LD, Shepherd RE (1994) Prior exercise suppresses the plasma tumor necrosis factor response to bacterial lipopolysaccharide. J Appl Physiol 77:1542–1547

Bak RPM, Nieuwland G, Meesters EH (2005) Coral reef crisis in deep and shallow reefs: 30 years of constancy and change in reefs of Curacao and Bonaire. Coral Reefs 24:475–479

Baythavong BS (2011) Linking the spatial scale of environmental variation and the evolution of phenotypic plasticity: Selection favors adaptive plasticity in fine-grained environments. Am Nat 178:75–87

Bensoussan N, Romano JC, Harmelin JG, Garrabou J (2010) High resolution characterization of northwest Mediterranean coastal waters thermal regimes: To better understand responses of benthic communities to climate change. Estuar Coast Shelf Sci 87:431–441

Bindea G, Mlecnik B, Hackl H, Charoentong P, Tosolini M, Kirilovsky A, Fridman W-H, Pagès F, Trajanoski Z,

Galon J (2009) ClueGO: a Cytoscape plug-in to decipher functionally grouped gene ontology and pathway annotation networks. Bioinformatics 25:1091–1093
Bongaerts P, Ridgway T, Sampayo EM, Hoegh-Guldberg O (2010) Assessing the "deep reef refugia" hypothesis: Focus on Caribbean reefs. Coral Reefs 29:309–327
Bramanti L, Manea E, Giordano B, Estaque T, Bianchimani O, Richaume J, Merigot B, Schull Q, Sartoretto S, Garrabou J, Guizen K (2023) The deep vault: a temporary refuge for temperate gorgonian forests facing marine heat waves. Mediterr Mar Sci 24:601–609
Brener-Raffall K, Vidal-Dupiol J, Adjeroud M, Rey O, Romans P, Bonhomme F, Pratlong M, Haguenauer A, Pillot R, Feuillassier L, Claereboudt M, Magalon H, Gélin P, Pontarotti P, Aurelle D, Mitta G, Toulza E (2019) Transcriptomics of thermal stress response in corals. Peer Community Ecol 100028
Conesa A, Götz S, García-Gómez JM, Terol J, Talón M, Robles M (2005) Blast2GO: A universal tool for annotation, visualization and analysis in functional genomics research. Bioinformatics 21:3674–3676
Cooper TF, Ulstrup KE, Dandan SS, Heyward AJ, Kühl M, Muirhead A, O'Leary RA, Ziersen BEF, van Oppen MJH (2011) Niche specialization of reef-building corals in the mesophotic zone: Metabolic trade-offs between divergent Symbiodinium types. Proc R Soc B Biol Sci 278:1840–1850
Costantini F, Rossi S, Pintus E, Cerrano C, Gili JM, Abbiati M (2011) Low connectivity and declining genetic variability along a depth gradient in Corallium rubrum populations. Coral Reefs 30:991–1003
Császár NBM, Seneca FO, Van Oppen MJH (2009) Variation in antioxidant gene expression in the scleractinian coral Acropora millepora under laboratory thermal stress. Mar Ecol Prog Ser 392:93–102
Deerenberg C, Arpanius V, Daan S, Bos N (1997) Reproductive effort decreases antibody responsiveness. Proc R Soc B Biol Sci 264:1021–1029
Demas GE, Chefer V, Talan MI, Nelson RJ (1997) Metabolic costs of mounting an antigen-stimulated immune response in adult and aged C57BL/6J mice. Am J Physiol Integr Comp Physiol 273:R1631–R1637
Desalvo MK, Sunagawa S, Voolstra CR, Medina M (2010) Transcriptomic responses to heat stress and bleaching in the elkhorn coral Acropora palmata. Mar Ecol Prog Ser 402:97–113
Desalvo MK, Voolstra CR, Sunagawa S, Schwarz JA, Stillman JH, Coffroth MA, Szmant AM, Medina M (2008) Differential gene expression during thermal stress and bleaching in the Caribbean coral Montastraea faveolata. Mol Ecol 17:3952–3971
Dixon G, Abbott E, Matz M (2020) Meta-analysis of the coral environmental stress response: Acropora corals show opposing responses depending on stress intensity. Mol Ecol 29:2855–2870
Drake JL, Mass T, Haramaty L, Zelzion E, Bhattacharya D, Falkowski PG (2013) Proteomic analysis of skeletal organic matrix from the stony coral stylophora pistillata. Proc Natl Acad Sci U S A 110:3788–3793
Enrichetti F, Dominguez-Carrió C, Toma M, Bavestrello G, Betti F, Canese S, Bo M (2019) Megabenthic communities of the Ligurian deep continental shelf and shelf break (NW Mediterranean Sea). PLoS One 14:
Estaque T, Richaume J, Bianchimani O, Schull Q, Mérigot B, Bensoussan N, Bonhomme P, Vouriot P, Sartoretto S, Monfort T, Basthard-Bogain S, Fargetton M, Gatti G, Barth L, Cheminée A, Garrabou J (2023) Marine heatwaves on the rise: One of the strongest ever observed mass mortality event in temperate gorgonians. Glob Chang Biol 29:6159–6162
Ferrier-Pagès C, Tambutté E, Zamoum T, Segonds N, Merle PL, Bensoussan N, Allemand D, Garrabou J, Tambutté S (2009) Physiological response of the symbiotic gorgonian Eunicella singularis to a longterm temperature increase. J Exp Biol 212:3007–3015
Garrabou J, Coma R, Bensoussan N, Bally M, Chevaldonné P, Cigliano M, Diaz D, Harmelin JG, Gambi MC, Kersting DK, Ledoux JB, Lejeusne C, Linares C, Marschal C, Pérez T, Ribes M, Romano JC, Serrano E, Teixido N, Torrents O, Zabala M, Zuberer F, Cerrano C (2009) Mass mortality in Northwestern Mediterranean rocky benthic communities: Effects of the 2003 heat wave. Glob Chang Biol 15:1090–1103
Garrabou J, Gómez-Gras D, Medrano A, Cerrano C, Ponti M, Schlegel R, Bensoussan N, Turicchia E, Sini M, Gerovasileiou V, Teixido N, Mirasole A, Tamburello L, Cebrian E, Rilov G, Ledoux J, Souissi J Ben, Khamassi F, Ghanem R, Benabdi M, Grimes S, Ocaña O, Bazairi H, Hereu B, Linares C, Kersting DK, la Rovira G, Ortega J, Casals D, Pagès-Escolà M, Margarit N, Capdevila P, Verdura J, Ramos A, Izquierdo A, Barbera C, Rubio-Portillo E, Anton I, López-Sendino P, Díaz D, Vázquez-Luis M, Duarte C, Marbà N, Aspillaga E, Espinosa F, Grech D, Guala I, Azzurro E, Farina S, Cristina Gambi M, Chimienti G, Montefalcone M, Azzola A, Mantas TP, Fraschetti S, Ceccherelli G, Kipson S, Bakran-Petricioli T, Petricioli D, Jimenez C, Katsanevakis S, Kizilkaya IT, Kizilkaya Z, Sartoretto S, Elodie R, Ruitton S, Comeau S, Gattuso J, Harmelin J (2022) Marine heatwaves drive recurrent mass mortalities in the Mediterranean Sea. Glob Chang Biol 28:5708–5725
Garrabou J, Perez T, Sartoretto S, Harmelin JG (2001) Mass mortality event in red coral Corallium rubrum populations in the Provence region (France, NW Mediterranean). Mar Ecol Prog Ser 217:263–272
Glynn PW (1996) Coral reef bleaching: Facts, hypotheses and implications. Glob Chang Biol 2:495–509
Gómez-Gras D, Linares C, Dornelas M, Madin JS, Brambilla V, Ledoux JB, López-Sendino P, Bensoussan N,

Garrabou J (2021) Climate change transforms the functional identity of Mediterranean coralligenous assemblages. Ecol Lett 24:1038–1051
Grenier, Marie, Idan T, Chevaldonné P, Pérez T (2023) Mediterranean marine keystone species on the brink of extinction. Glob Chang Biol 1–3
Haguenauer A, Zuberer F, Ledoux JB, Aurelle D (2013) Adaptive abilities of the Mediterranean red coral Corallium rubrum in a heterogeneous and changing environment: From population to functional genetics. J Exp Mar Bio Ecol 449:349–357
Heck M, Neely BA (2020) Proteomics in Non-model Organisms: A New Analytical Frontier. J Proteome Res 19:3595–3606
Hughes L (2000) Biological consequences of global warming: Is the signal already apparent? Trends Ecol Evol 15:56–61
Jin L, Bi Y, Hu C, Qu J, Shen S, Wang X, Tian Y (2021) A comparative study of evaluating missing value imputation methods in label-free proteomics. Sci Rep 11:1–11
Jombart T, Devillard S, Balloux F (2010) Discriminant analysis of principal components: a new method for the analysis of genetically structured populations. BMC Genet 11:94
Kenkel CD, Matz M V. (2017) Gene expression plasticity as a mechanism of coral adaptation to a variable environment. Nat Ecol Evol 1:1–6
Langfelder P, Horvath S (2008) WGCNA: An R package for weighted correlation network analysis. BMC Bioinformatics 9:
Ledoux JB, Aurelle D, Bensoussan N, Marschal C, Féral JP, Garrabou J (2015) Potential for adaptive evolution at species range margins: Contrasting interactions between red coral populations and their environment in a changing ocean. Ecol Evol 5:1178–1192
Ledoux JB, Mokhtar-Jamaï K, Roby C, Féral JP, Garrabou J, Aurelle D (2010) Genetic survey of shallow populations of the Mediterranean red coral [Corallium rubrum (Linnaeus, 1758)]: New insights into evolutionary processes shaping nuclear diversity and implications for conservation. Mol Ecol 19:675–690
Lesser MP (2006) Oxidative stress in marine environments: Biochemistry and Physiological Ecology. Annu Rev Physiol 68:253–278
Lesser MP, Marc S, Michael S, Michiko O, Gates RD, Andrea G (2010) Photoacclimatization by the coral Montastraea cavernosa in the mesophotic zone: Light, food, and genetics. Ecology 91:990–1003
Linares C, Coma R, Garrabou J, Díaz D, Zabala M (2008) Size distribution, density and disturbance in two Mediterranean gorgonians: Paramuricea clavata and Eunicella singularis. J Appl Ecol 45:688–699
Malik A, Einbinder S, Martinez S, Tchernov D, Haviv S, Almuly R, Zaslansky P, Polishchuk I, Pokroy B, Stolarski J, Mass T (2021) Molecular and skeletal fingerprints of scleractinian coral biomineralization: From the sea surface to mesophotic depths. Acta Biomater 120:263–276
Martínez-Quintana A, Bramanti L, Viladrich N, Rossi S, Guizien K (2015) Quantification of larval traits driving connectivity: the case of Corallium rubrum (L. 1758). Mar Biol 162:309–318
Masmoudi MB, Chaoui L, Topçu NE, Hammami P, Kara MH, Aurelle D (2016) Contrasted levels of genetic diversity in a benthic Mediterranean octocoral: Consequences of different demographic histories? Ecol Evol 6:8665–8678
Mayfield AB, Wang Y Bin, Chen CS, Chen SH, Lin CY (2016) Dual-compartmental transcriptomic + proteomic analysis of a marine endosymbiosis exposed to environmental change. Mol Ecol 25:5944–5958
Noël C, Cuzin P, Cormier A, Leroi L, Durand P (2021) ORSON: workflow for prOteome and tRanScriptome functiOnal aNnotation. WorkflowHub
Oliver ECJ, Donat MG, Burrows MT, Moore PJ, Smale DA, Alexander L V., Benthuysen JA, Feng M, Sen Gupta A, Hobday AJ, Holbrook NJ, Perkins-Kirkpatrick SE, Scannell HA, Straub SC, Wernberg T (2018) Longer and more frequent marine heatwaves over the past century. Nat Commun 9:1324
Pasqueron de Fommervault O, Migon C, D'Ortenzio F, Ribera d'Alcalà M, Coppola L (2015) Temporal variability of nutrient concentrations in the northwestern Mediterranean sea (DYFAMED time-series station). Deep Res Part I Oceanogr Res Pap 100:1–12
Pey A, Catanéo J, Forcioli D, Merle PL, Furla P (2013) Thermal threshold and sensitivity of the only symbiotic Mediterranean gorgonian Eunicella singularis by morphometric and genotypic analyses. Comptes Rendus - Biol 336:331–341
Pinzón JH, Kamel B, Burge CA, Harvell CD, Medina M, Weil E, Mydlarz LD (2015) Whole transcriptome analysis reveals changes in expression of immune-related genes during and after bleaching in a reef-building coral. R Soc Open Sci 2:
Pivotto ID, Nerini D, Masmoudi M, Kara H, Chaoui L, Aurelle D (2015) Highly contrasted responses of Mediterranean octocorals to climate change along a depth gradient. R Soc Open Sci 2:
Pratlong M, Haguenauer A, Chabrol O, Klopp C, Pontarotti P, Aurelle D (2015) The red coral (Corallium rubrum) transcriptome: A new resource for population genetics and local adaptation studies. Mol Ecol Resour 15:1205–1215

Previati M, Scinto A, Cerrano C, Osinga R (2010) Oxygen consumption in Mediterranean octocorals under different temperatures. J Exp Mar Bio Ecol 390:39–48
Prioux C, Tignat-Perrier R, Gervais O, Estaque T, Schull Q, Reynaud S, Béraud E, Mérigot B, Beauvieux A, Marcus M-I, Richaume J, Bianchimani O, Cheminée A, Allemand D, Ferrier-Pagès C (2023) Unveiling microbiome changes in Mediterranean octocorals during the 2022 marine heatwaves: quantifying key bacterial symbionts and potential pathogens. Microbiome 11:271
Quevillon E, Silventoinen V, Pillai S, Harte N, Mulder N, Apweiler R, Lopez R (2005) InterProScan: protein domains identifier. Nucleic Acids Res 33:W116–W120
R Core Team (2021) R: A Language and Environment for Statistical Computing.
Råberg L, Grahn M, Hasselquist D, Svensson E (1998) On the adaptive significance of stress-induced immunosuppression. Proc R Soc London Ser B Biol Sci 265:1637–1641
Raftos DA, Kuchel R, Aladaileh S, Butt D (2014) Infectious microbial diseases and host defense responses in Sydney rock oysters. Front Microbiol 5:1–12
Ranz JM, Machado CA (2006) Uncovering evolutionary patterns of gene expression using microarrays. Trends Ecol Evol 21:29–37
Reusch TBH (2014) Climate change in the oceans: Evolutionary versus phenotypically plastic responses of marine animals and plants. Evol Appl 7:104–122
Shannon P, Markiel A, Ozier O, Baliga NS, Wang JT, Ramage D, Amin N, Schwikowski B, Ideker T (2003) Cytoscape: A Software Environment for Integrated Models of Biomolecular Interaction Networks. Genome Res 13:2498–2504
Sini M, Kipson S, Linares C, Koutsoubas D, Garrabou J (2015) The yellow gorgonian Eunicella cavolini: Demography and disturbance levels across the Mediterranean Sea. PLoS One 10:
Smith KE, Burrows MT, Hobday AJ, King NG, Moore PJ, Sen Gupta A, Thomsen MS, Wernberg T, Smale DA (2023) Biological Impacts of Marine Heatwaves. Ann Rev Mar Sci 15:119–145
Tambutté E, Venn AA, Holcomb M, Segonds N, Techer N, Zoccola D, Allemand D, Tambutté S (2015) Morphological plasticity of the coral skeleton under CO2-driven seawater acidification. Nat Commun 6:
Tignat-Perrier R, van de Water JAJM, Guillemain D, Aurelle D, Allemand D, Ferrier-Pagès C (2022) The Effect of Thermal Stress on the Physiology and Bacterial Communities of Two Key Mediterranean Gorgonians. Appl Environ Microbiol 88:
Tomanek L (2014) Proteomics to study adaptations in marine organisms to environmental stress. J Proteomics 105:92–106
Vargas S, Zimmer T, Conci N, Lehmann M, Wörheide G (2022) Transcriptional response of the calcification and stress response toolkits in an octocoral under heat and pH stress. Mol Ecol 31:798–810

Figure Captions

Figure 1. In situ thermal regime. (a) Time series of daily maximum seawater temperature of the station Riou Sud, located at a distance of 600m to the transplanting site Imperial du large at Marseille data (provided by T-MedNet.org) (NW Mediterranean Sea) over a year (January 2021-2022). The reciprocal transplantation experiment began mid-June and ended mid-November 2021 (white dotted lines). Data were provided by the regional temperature observation network T-MEDNet, www.t-mednet.org, site Marseille Riou-sud, Dorian Guillemain, OSU Institut Pytheas UMS 3470. (b) Number of days presenting a temperature over a given value between 20 °C to 25 °C (daily maximum temperature) at 5m (purple), 20m (orange) and 40m (green) depth along the experiment. Black contour represents temperatures exceeding 25°C.

Figure 2. Reciprocal transplant design. In June 2021, 16 colonies of *E. cavolini* were reciprocally transplanted between shallow (20m) and mesophotic zones (70m). At the end of the experiment (November 2021), 4 treatments

were obtained: colony fragments retained at native depth (C_{20} and C_{70}) and colony fragments transplanted in shallow/mesophotic zones ($T_{70\rightarrow20}$ and $T_{20\rightarrow70}$). A single colony provided one control (C) and one transplant (T).

Figure 3. Protein expression plasticity in transplanted gorgonians based on DAPC analysis on the scaled matrix of protein intensities (all identified and filtered proteins). The *x* axis is the direction along which the difference between control Mesophotic and Shallow gorgonians is maximized (discriminant function which explained 43% of total variance). The curves are density plots of the four treatments. Blue and Yellow indicates gorgonians originating from mesophotic and shallow reefs respectively; solid fills indicate control groups, whereas transparent fills represent transplants. Arrows indicate the extent of protein expression shifts upon transplantation.

Figure 4. Hierarchical clustering dendrogram of module eigengenes and heatmap of spearman's correlations coefficients between module eigengenes (rows) and treatment (columns). Values with module names indicates the number of proteins belonging to each module.

Figure 5. Gene Ontology (GO) enrichment analysis of WGCNA protein in "brown" module for $T_{20\rightarrow70}$ vs C_{20}. (a) Hierarchical clustering of enriched biological process gene ontology terms among proteins in the brown module. *FDR<0.1, **FDR<0.05, ***FDR<0.01). Fractions indicate the number of proteins that are differentially regulated. (b) Enrichment analysis of the 8 enriched GO terms. Blue dots show a protein underexpressed in colonies $T_{20\rightarrow70}$ vs C_{20}, red dots indicate protein overexpressed. Z-score=(upregulated–downregulated)/√(upregulated+downregulated).

Figure 6. ClueGO analysis of biological process significantly enriched (FDR < 0.1) in at least one treatment comparison. Node size correspond to the statistical significance (FDR).

Figure 7. Gene Ontology (GO) enrichment analysis using protein' Gene Significance. (a) and (b) Hierarchical clustering of enriched biological process gene ontology. *FDR<0.1, ** FDR<0.05, *** FDR<0.01. Fractions indicate the number of proteins that are differentially regulated. (c) and (d) GO circle plot displaying enrichment analysis for the first 10 GO terms with lowest FDR. Blue dots showed a protein underexpressed in colonies

$T_{70\rightarrow20}$ (c) $T_{20\rightarrow70}$ (d) to their respective control, red dot indicated protein overexpressed. The outer to inner layers of grey circles indicated the relative fold-change of gene expression (from higher to lower). Z-score=(upregulated–downregulated)/√(upregulated+downregulated).

Figures

Figure 1.

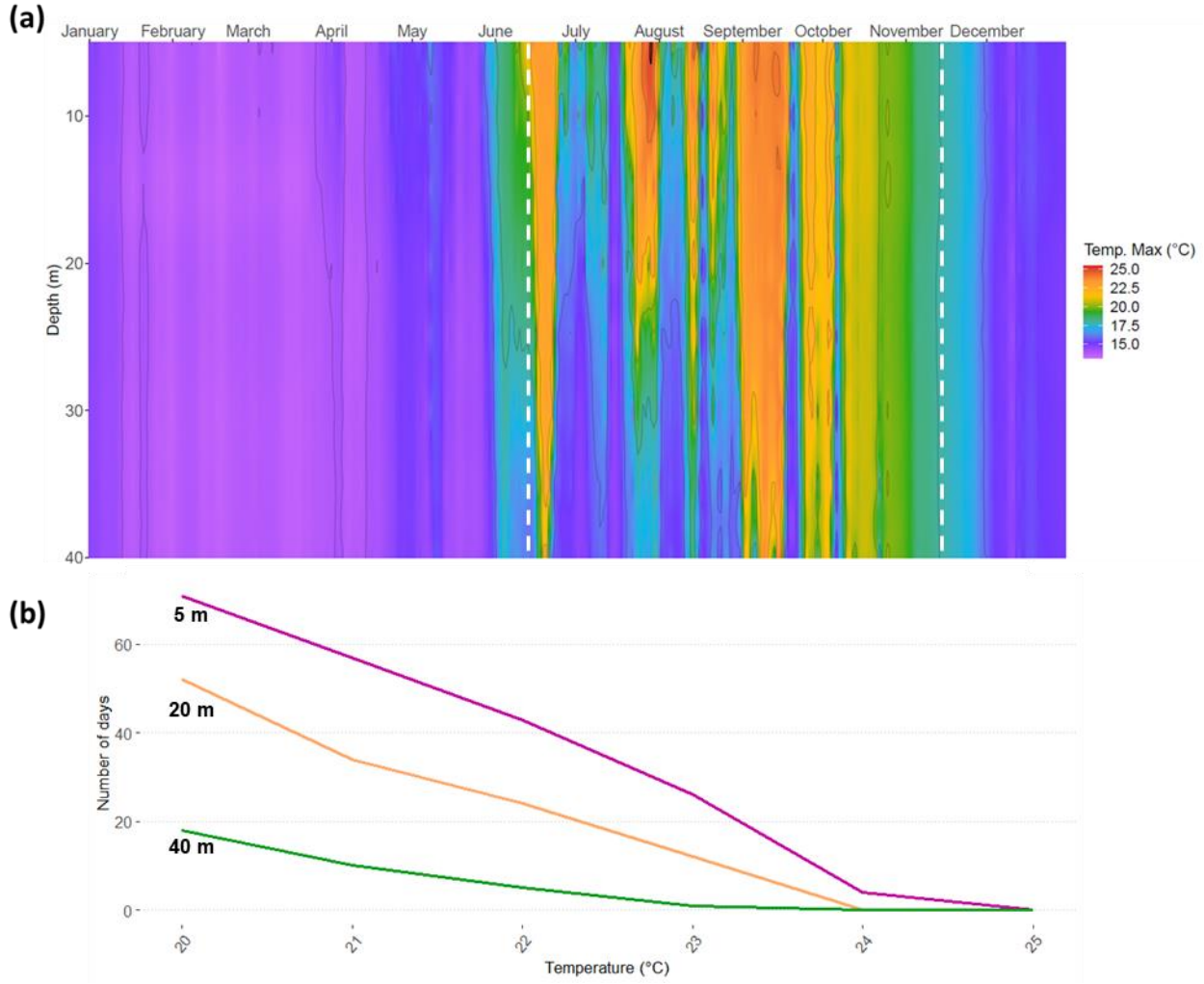

Figure 2.

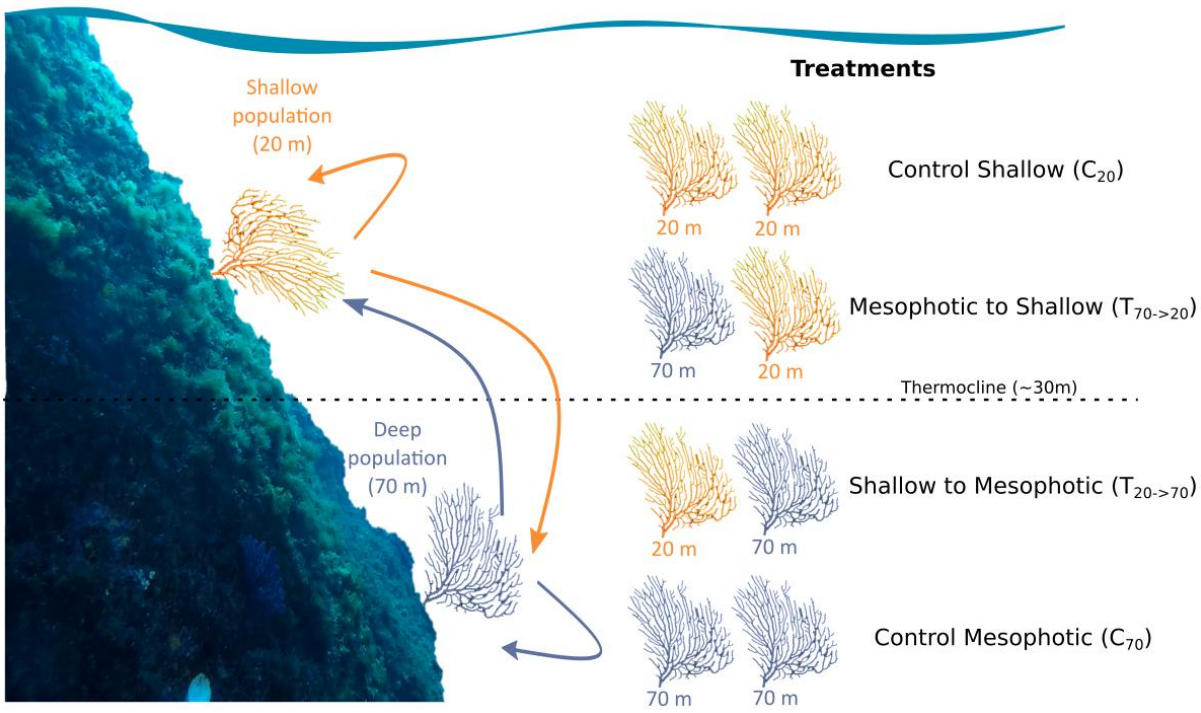

Figure 3.

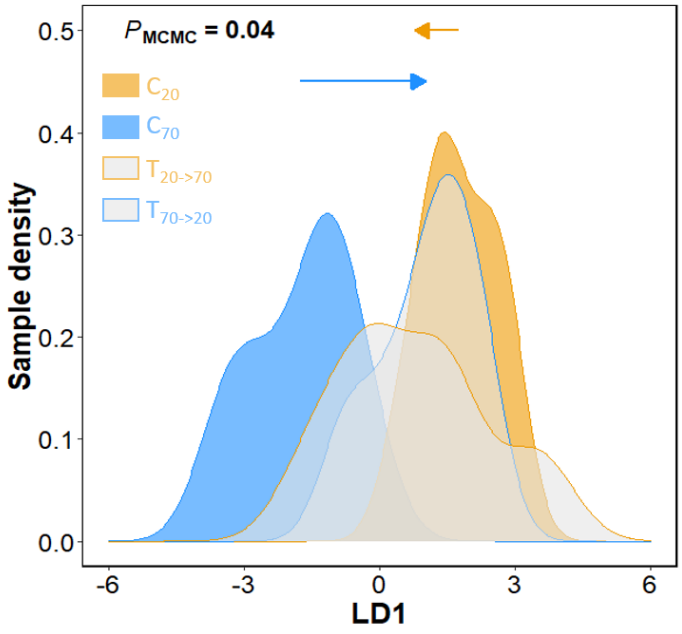

Figure 4.

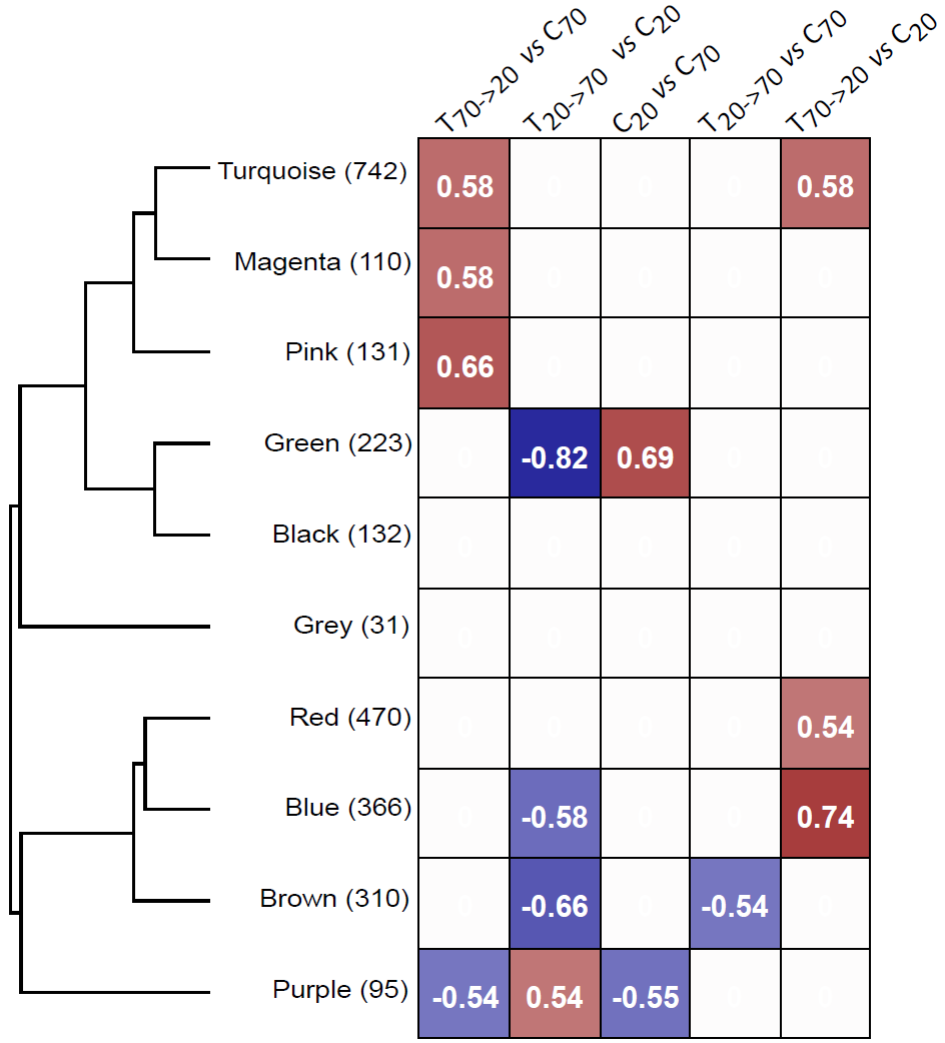

Figure 5.

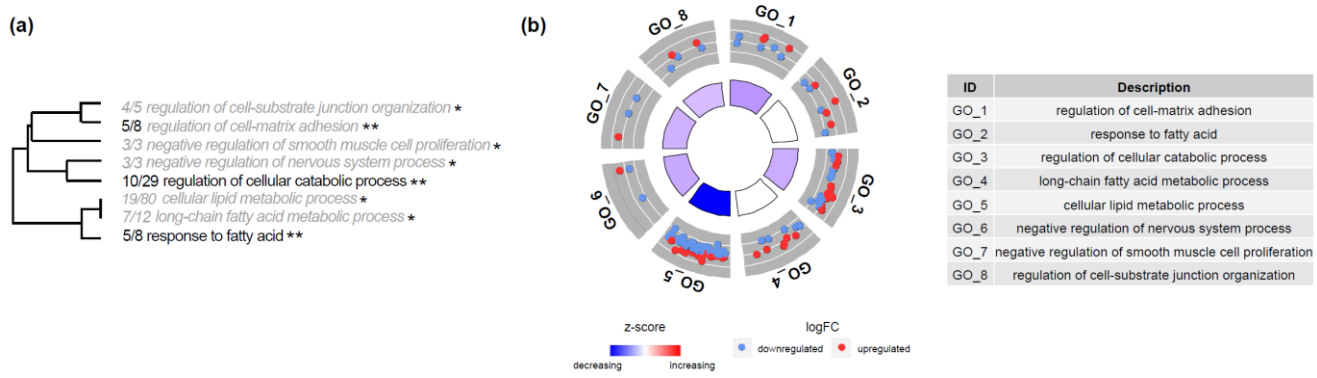

ID	Description
GO_1	regulation of cell-matrix adhesion
GO_2	response to fatty acid
GO_3	regulation of cellular catabolic process
GO_4	long-chain fatty acid metabolic process
GO_5	cellular lipid metabolic process
GO_6	negative regulation of nervous system process
GO_7	negative regulation of smooth muscle cell proliferation
GO_8	regulation of cell-substrate junction organization

Figure 6

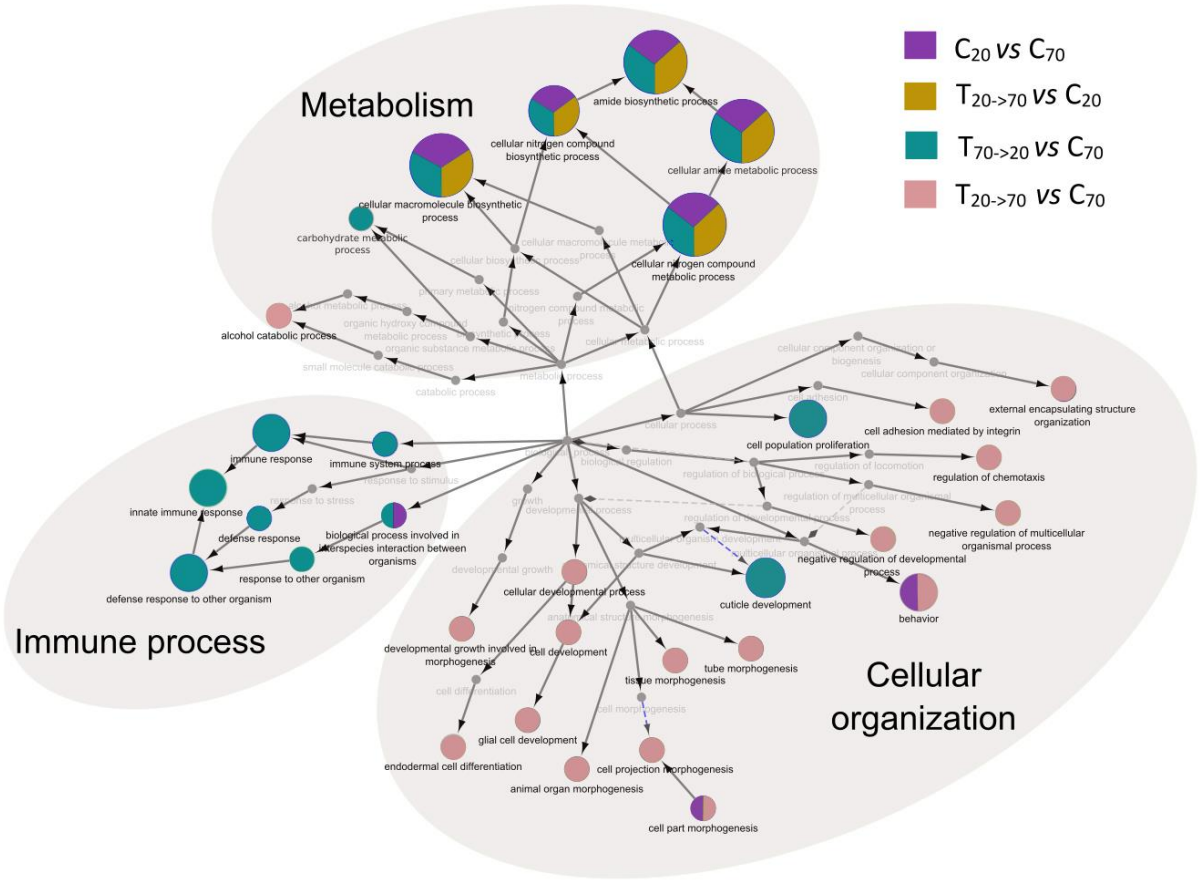
C20 vs C70
T20->70 vs C20
T70->20 vs C70
T20->70 vs C70
Metabolism
amide biosynthetic process
cellular nitrogen compound biosynthetic process
cellular amide metabolic process
cellular macromolecule biosynthetic process
carbohydrate metabolic process
cellular nitrogen compound metabolic process
alcohol catabolic process
Immune process
immune response
immune system process
innate immune response
defense response
biological process involved in interspecies interaction between organisms
response to other organism
defense response to other organism
Cellular organization
cell population proliferation
cell adhesion mediated by integrin
external encapsulating structure organization
regulation of chemotaxis
negative regulation of multicellular organismal process
negative regulation of developmental process
behavior
cuticle development
cellular developmental process
developmental growth involved in morphogenesis
cell development
tube morphogenesis
tissue morphogenesis
glial cell development
endodermal cell differentiation
cell projection morphogenesis
animal organ morphogenesis
cell part morphogenesis

Figure 7.

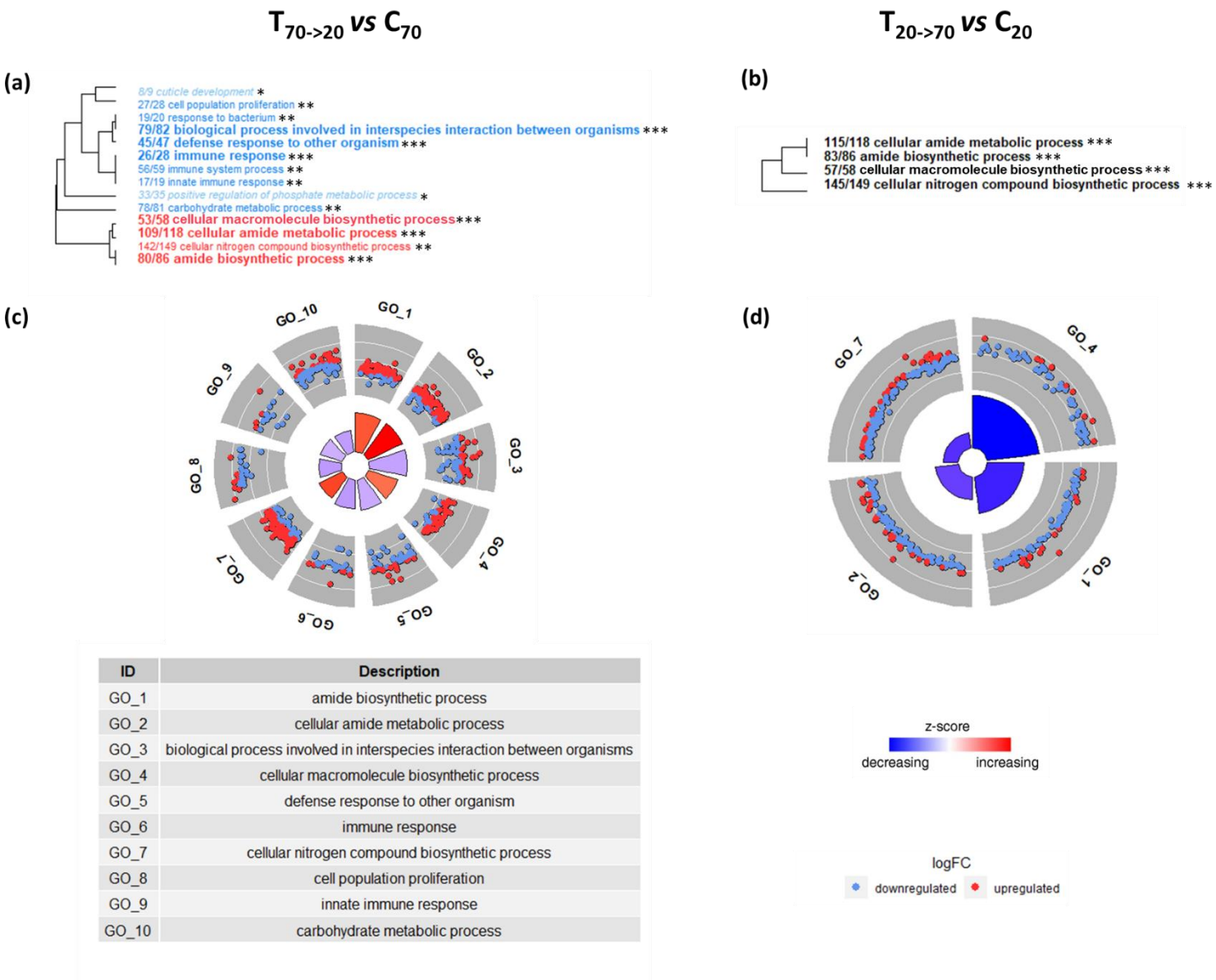

ID	Description
GO_1	amide biosynthetic process
GO_2	cellular amide metabolic process
GO_3	biological process involved in interspecies interaction between organisms
GO_4	cellular macromolecule biosynthetic process
GO_5	defense response to other organism
GO_6	immune response
GO_7	cellular nitrogen compound biosynthetic process
GO_8	cell population proliferation
GO_9	innate immune response
GO_10	carbohydrate metabolic process

Supporting information

Mesophotic zone as refuge: acclimation and in-depth physiological response of yellow gorgonians in the Mediterranean Sea

Anaïs Beauvieux[1], Bastien Mérigot[1], Jérémy Le Luyer[2], Jean-Marc Fromentin[1], Nathan Couffin[3,4], Adrien Brown[3,4], Olivier Bianchimani[5], Régis Hocdé[1], Didier Aurelle[6], Jean-Baptiste Ledoux[7], Fabrice Bertile[3,4], Quentin Schull[1]

Affiliations :

[1] MARBEC, Univ Montpellier, CNRS, Ifremer, IRD, Sète, France

[2] Ifremer, IRD, Institut Louis-Malardé, Univ. Polynésie française, EIO, F-98719 Taravao, Tahiti, Polynésie française, France

[3] Université de Strasbourg, CNRS, IPHC UMR 7178, 23 rue du Loess, 67037, Strasbourg Cedex 2, France

[4] Infrastructure Nationale de Protéomique ProFI, FR2048 CNRS CEA, Strasbourg 67087, France

[5] Septentrion Environnement, Marseille, France

[6] Aix Marseille Univ., Université de Toulon, CNRS, IRD, MIO, Marseille, France

[7] CIIMAR/CIMAR, Centro Interdisciplinar de Investigação Marinha e Ambiental, Universidade do Porto, Porto, Portugal.

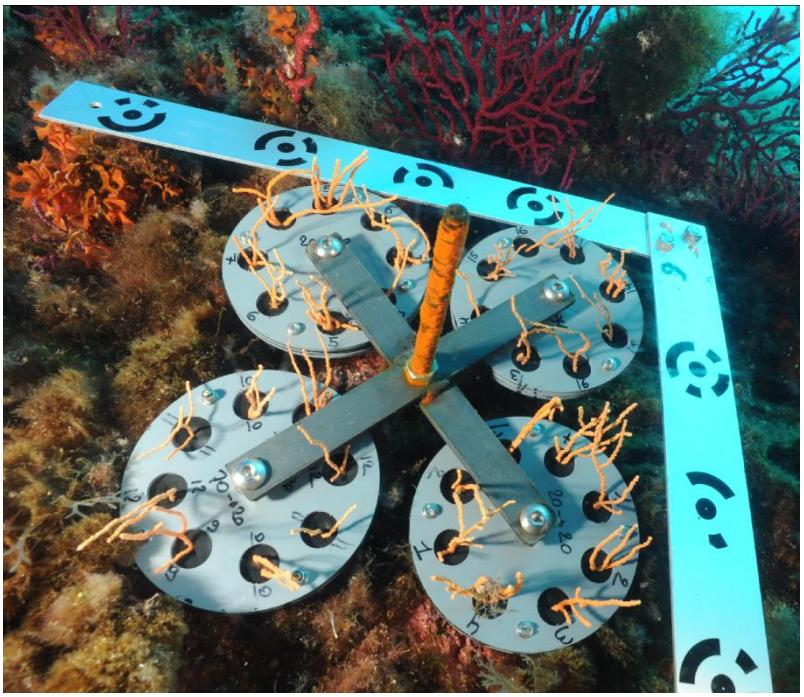

ESM2: Picture of one of the experimental plate. The apical tips of around 5 cm in length of 4 fragments per colony of *Eunicella cavolini* were randomly sampled via closed-circuit rebreather and fixed underwater.

ESM3. Quantitative proteomic analysis of *Eunicella cavolini* samples

Protein extraction

Frozen samples were ground under liquid nitrogen using a ball mill (MM400, Retsch, Eragny sur Oise, France), and the resulting powder was used to extract total protein by sonication at 25°C for 10 cycles of 30 seconds using a Bioruptor Pico (Diagenode, Denville, NJ, USA) in a lysis buffer (urea 6M, thiourea 2M, ammonium bicarbonate 0.1M, protease inhibitors 1/100). After centrifugation (30s, 2000 x g, room temperature) to pellet remaining cell debris, protein concentration was determined using Pierce 660-nm Protein Assay Reagent (Thermofisher, Rockford, IL, USA). At this stage, a reference sample comprising an equal volume of all protein extracts was made, to be injected regularly during the whole experiment and thus allow QC-related measurements.

Twenty-five µg of each sample were loaded onto SDS-PAGE stacking gels (4% polyacrylamide) and electrophoresis was performed for 20 minutes at 50V. After protein fixation (50% ethanol, 3% phosphoric acid) during 20 min, staining using colloidal Coomassie Blue (30 min) allowed visualization of a stacked protein band that was excised from the gel. Destaining was performed using 50% acetonitrile/ 50% ammonium hydrogen carbonate 25 mM, and dehydration using pure acetonitrile. Proteins were then reduced and alkylated in-gel using 10 mM DTT in 25 mM ammonium hydrogen carbonate (30 minutes at 60°C then 15 minutes at room temperature) and 55 mM iodoacetamide in 25 mM ammonium hydrogen carbonate (30 minutes at room temperature in the dark), respectively. Gel pieces were washed using 25 mM ammonium hydrogen carbonate (5 minutes at room temperature) then acetonitrile (5 minutes at room temperature), and these steps were repeated 6 times. Finally, dehydration used acetonitrile (2 x 5 minutes at room temperature), and in-gel digestion of proteins was performed overnight at 37°C using trypsin/Lys-C (Promega, Madison, WI, USA; 500 ng per band). After trypsin/Lys-C digestion, the resulting peptides were extracted at 100 rpm on an orbital shaker during 3 hours using 80% acetonitrile/0.1% formic acid in water, then they were vacuum-dried (SpeedVac, Savant, Thermoscientific, Waltham, MA, USA) and suspended in 250 µL of H_2O/acetonitrile (98/2), 0.1% formic acid. At this stage, a set of reference peptides (iRT kit; Biognosys AG, Schlieren, Switzerland) was added to peptide extracts (1µL/9µL of sample) for QC-related measurements.

MS/MS analysis

Samples were analyzed on a nanoUPLC-system (nano-Acquity, Waters, Milford, MA, USA) coupled to a quadrupole-Orbitrap hybrid mass spectrometer (Q-Exactive HF-X, Thermo Scientific, San Jose, CA, USA). The system was fully controlled by XCalibur software (v4.0.27.9; Thermo Fisher Scientific). Concentration/desalting was first performed by loading of 2 µL of sample on a Symmetry C18 trap column (100Å, 5 µm, 180 µm × 20 mm; Waters) using 99% of formic acid 0.1% in water (solvent A) and 1% of formic acid 0.1% in acetonitrile (solvent B) at a flow rate of 5 µl/min for 3 min. Peptide elution was then performed using a nanoEase M/Z Peptide BEH C18 column (130Å, 1.7 µm, 75 µm X 250 mm, Waters) maintained at 60°C while applying a solvent gradient from 2% to 25% of B in 77 minutes then from 25% to 35% in 10 minutes at a flow rate of 350 nL/min. To reduce carry-over, the column was washed using acetonitrile 90% for 5 minutes then a solvent blank was run in between each sample.

The Q-Exactive HF-X was operated in positive ion mode with the source temperature set to 250°C and spray voltage to 1.9 kV. Full-scan MS spectra (375-1500 m/z) were acquired at a resolution of 120,000 at m/z 200, with a maximum injection time set to 60 ms and an AGC target value set to $3x10^6$ charges. The lock-mass option was enabled (polysiloxane, 445.12002 m/z). Up to 20 most intense peptides (at least doubly charged) per full scan were isolated using a 2 m/z window and they were

fragmented using higher-energy collisional dissociation (normalized collision energy set to 27 and dynamic exclusion of already fragmented precursors set to 60 s). MS/MS spectra (300-2000 m/z) were acquired with a resolution of 15,000 at m/z 200, with a maximum injection time of 60 ms and an AGC target value set to $1x10^5$ and the peptide match selection option was turned on. Peak intensities and retention times of reference peptides were monitored in a daily fashion.

Raw data processing

MS raw data processing was performed in MaxQuant software (v2.0.3.1). Peak lists were searched using Andromeda search engine implemented in MaxQuant. The protein database contained protein sequences from a home-made annotation of *Eunicella cavolini* RNA sequencing data (NCBI BioProject PRJNA249058, 8 different RNAseq datasets). Briefly, reads were downloaded (SRA toolkit v2.11.0) and assembled into transcripts (Trinity v2.13.2 default parameters). Transdecoder v5.5.0 was used to predict the ORFs evaluated as "likely coding region" using default parameters. Finally, 51,038 protein sequences were obtained after translation and redundancy removal. A blast search strategy using Blast+ v2.12.0 (NCBI) enabled us to attribute a name to these translated sequences. Blast searches first considered the species phylogenetically the closest to *E. cavolini*. Using a minimum bit-score threshold set to 50, only the best blast hit found in UniprotKB (accessed in March 2022) was retained for a given *E. cavolini* protein, allowing protein name propagation. If no satisfying blast hit was found, another blast search was performed against UniprotKB protein sequences from species phylogenetically progressively more distant to *E. cavolini*. Sequences of common contaminants (247 entries; contaminants.fasta included in MaxQuant) were added to the obtained protein database as well as decoy sequences (revert mode). The first search was performed using a precursor mass tolerance of 20 ppm, and 4.5 ppm for the main search after recalibration. Fragment ion mass tolerance was set to 20 ppm. The second peptide research option was enabled. Carbamidomethylation of cysteines was considered as a fixed modification and oxidation of methionines and acetylation of protein N-termini as variable modifications during the search. A maximum number of one missed cleavages was tolerated, and a false discovery rate (FDR) of 1% for both peptide spectrum matches (minimum length of seven amino acids) and proteins was accepted during identification. Only the proteins identified with at least two unique peptide were retained, and decoy hits and potential contaminants were removed.

Peptide quantification

Regarding quantification, data normalisation and protein abundance estimation were performed using the MaxLFQ (label-free quantification) option implemented in MaxQuant (Cox et al. 2014) using a "minimal ratio count" of one. The option "Match between runs" was enabled using a 0.7-minute time window after retention time alignment. Quantification was performed using unique peptides only. Both unmodified unique peptides and, if detected, also their modified counterpart (acetylation of protein N-termini and oxidation of methionines) were considered. All other MaxQuant parameters were set as default. The very few contaminants and reversed proteins that were identified were removed from the dataset. All proteins quantified with at least two unique peptides in at least 70% of individuals per treatments were kept for further analysis. No absent/present cases were recorded. The mass spectrometry proteomics data have been deposited to the ProteomeXchange Consortium via the PRIDE (Perez-Riverol et al. 2019) partner repository with the dataset identifier PXD037261.

QC-related measurements indicated stable performances of the analysis system all along the experiment, with a median coefficient of variation (CV) of 0.33% for retention times of iRT peptides over all injections, the median CV for their raw intensities being calculated at 11.1%. A median CV of only 9.6% for LFQ values of the proteins quantified from the repeated injections of the reference sample, and this value reached 27.5% on average for intragroup LFQ values of quantified proteins.

ESM4. Overview of proteome-wide change between treatments (Method)

Before WGCNA analysis, to obtain an overview of the magnitude of change (or similarity) of proteins expression between treatments, we used euKaryotic Orthologous Groups (KOGs) enrichment analysis using the '*KOGMWU*' package (https://github.com/cran/KOGMWU). KO categories are not hierarchical and have very little or no overlap in terms of proteins they involve (compared to GO terms), which allows the generation of compact functional summaries at the whole-proteome scale and the quantitative comparison of multiple datasets. The log2 Fold Changes (FC which is the relative ratio of each protein between two conditions), were used as measures of differential expression between two treatments. Enrichment of each KOG class with up- or down-regulated proteins was inferred based on the class' delta-rank and two-sided Mann-Whitney U test. Enrichment analysis between two control treatments (*Control Shallow vs Control Mesophotic* C_{20} *vs* C_{70}) provided information if these two population have similar or different phenotypes. Comparisons between transplanted gorgonians and their control (*Control Mesophotic vs Mesophotic to Shallow* C_{20} *vs* $T_{70->20}$ and *Control Shallow vs Shallow to Mesophotic* C_{70} *vs* $T_{20->70}$) described the consequences of transplantation to the transplants phenotype. Finally, comparisons of *Mesophotic to Shallow vs Control Shallow* $T_{70->20}$ *vs* C_{20} and *Shallow to Mesophotic vs Control Mesophotic* $T_{20->70}$ *vs* C_{70} presented if transplants had at the end of the experiment different or similar phenotypes to the population of their contrasted destination site.

Overview of proteome-wide change between treatments (Results)

- Control Shallow *vs* Control Mesophotic

Eukaryotic orthologous group (KOGs) analysis identified three KOG classes significantly enriched when comparing the control groups together (C_{20} *vs* C_{70}). Colonies from shallow waters significantly under-expressed proteins from KOG categories "Cell wall/membrane/envelope biogenesis" (FDR<0.1) and "Signal transduction mechanisms" (FDR<0.01) while proteins of "Translation, ribosomal structure and biogenesis" (FDR>0.01) were significantly overexpressed (ESM5a).

- Transplant vs Origin

Gorgonians transplanted in shallow waters significantly under-expressed proteins from "Carbohydrate transport and metabolism" (FDR<0.05) and "Amino acid transport and metabolism" (FDR<0.1) while "Intracellular trafficking, secretion, and vesicular transport" (FDR <0.05) and "Energy production and conversion" (FDR<0.1) were significantly over-expressed compared to their control ($T_{70->20}$ *vs* C_{70}, ESM5a). Moreover, gorgonians transplanted in Mesophotic water significantly overexpressed proteins from the KOG category "Translation, ribosomal structure and biogenesis" (FDR<0.05) compared to their control ($T_{20->70}$ *vs* C_{20}) (ESM5a). We also noted that proteins from the category "Nuclear structure" displayed the strongest difference in terms of expression for comparisons between transplants and their control despite being not-significantly enriched.

- Transplant vs destination

Comparison between transplanted gorgonian and the population of their destination depth presented contrasted results. In fact, while no KOG were significantly enriched in gorgonian transplanted to shallow waters ($T_{70->20}$ *vs* C_{20}), the opposite comparison ($T_{20->70}$ *vs* C_{70}) revealed three significantly enriched KOG classes (ESM5a). Proteins from "Extracellular structures" (FDR<0.1) and "Cell/membrane/envelope biogenesis" (FDR<0.05) were under-expressed while "Translation, ribosomal structure and biogenesis" (FDR<0.1) were overexpressed in transplants "Shallow to Mesophotic".

- Transplant vs transplant

Interestingly, colonies of both transplantation treatments (Mesophotic to Shallow and Shallow to Mesophotic) seemed to display an opposite response (KOG categories had opposite expression pattern, ie. a KOG category overexpressed when transplanted from shallow to Mesophotic was under-expressed in transplants from Mesophotic to shallow, ESM5a). This pattern is consistent with the comparison of the KOG delta-rank values (i.e., the high-level quantitative functional responses) between the two non-native transplants that showed a significant negative Spearman correlation ($cor = -0.63$, $p < 0.01$, ESM5b).

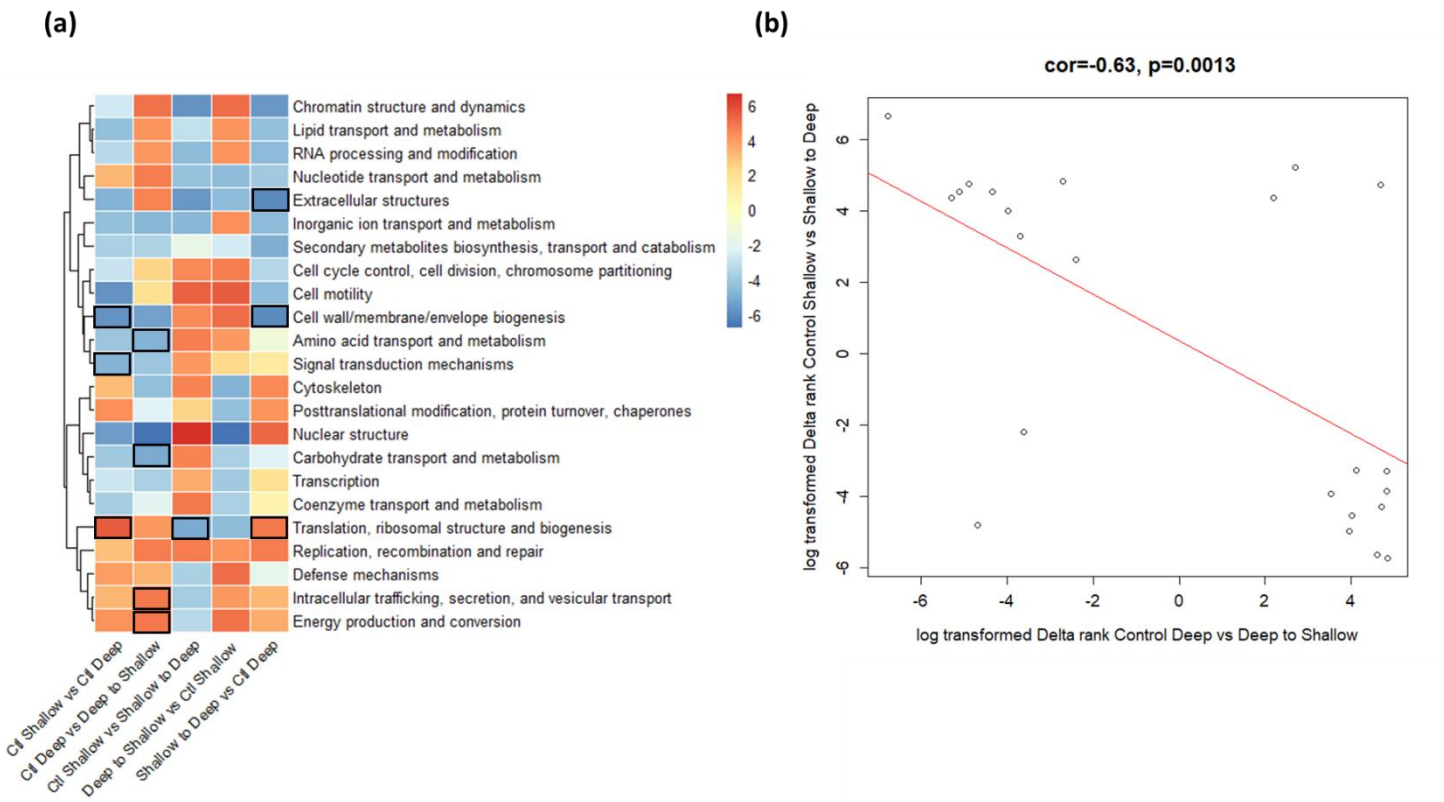

ESM5. Hierarchical clustering analyse of KOG term enrichments. (a) Displayed are the KOG delta ranks (which is the difference between the mean rank of proteins belonging to this KOG class and all other proteins). Darker red or blue colors indicate some KOG class are enriched with over- or under-expressed proteins. Boxes outlined in bold are statistically significant enrichment (FDR – adjusted pval < 0.1) within each comparison. (b)Correlation of KOG delta ranks between colonies from Control Mesophotic *vs* Mesophotic to Shallow and from Control Shallow *vs* Shallow to Mesophotic.

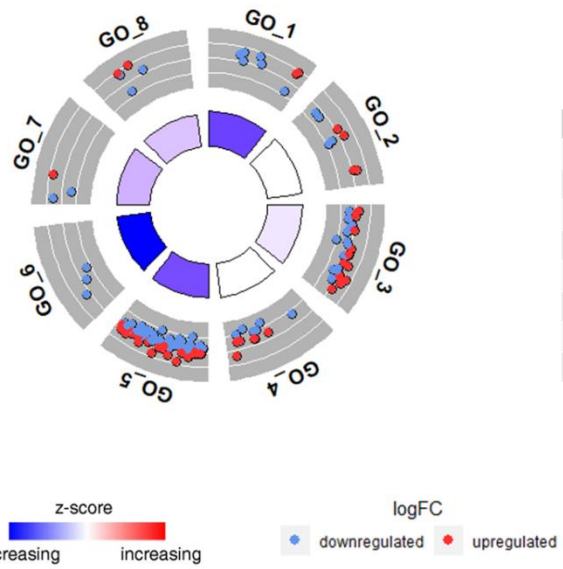

ID	Description
GO_1	regulation of cell-matrix adhesion
GO_2	response to fatty acid
GO_3	regulation of cellular catabolic process
GO_4	long-chain fatty acid metabolic process
GO_5	cellular lipid metabolic process
GO_6	negative regulation of nervous system process
GO_7	negative regulation of smooth muscle cell proliferation
GO_8	regulation of cell-substrate junction organization

ESM6. Gene Ontology (GO) enrichment analysis of WGCNA protein in “brown” module for Shallow to Mesophotic vs Control Mesophotic comparison. GO circle plot displaying enrichment analysis 8 enriched GO terms. Within each selected GO term, blue dot showed a protein underexpressed in colonies “Shallow to Mesophotic” compared to Control Mesophotic while red dot indicated protein overexpressed. The rectangle is coloured with the blue-red gradient according to the z-score. Z-score = (upregulated – downregulated) / √ (upregulated + downregulated).

(a)

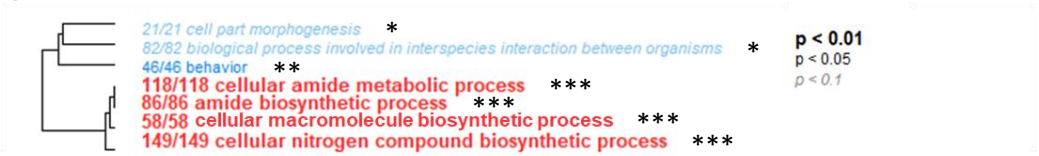

(b)

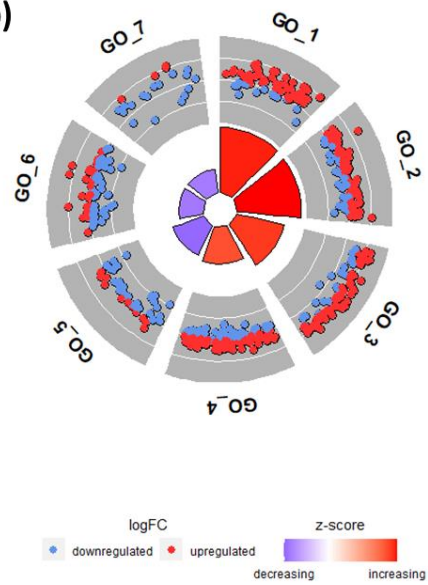

ID	Description
GO_1	cellular macromolecule biosynthetic process
GO_2	cellular amide metabolic process
GO_3	amide biosynthetic process
GO_4	cellular nitrogen compound biosynthetic process
GO_5	behavior
GO_6	biological process involved in interspecies interaction between organisms
GO_7	cell part morphogenesis

ESM7. Gene Ontology (GO) enrichment analysis based on proteins Gene Significance. (a) Hierarchical clustering of enriched biological process gene ontology terms among proteins with the highest gene significance for the comparison Control Shallow vs Control Mesophotic. Font size indicates the level of FDR-adjusted statistical significance. Term names are preceded by a fraction indicating the number of individual proteins within each term that are differentially regulated. (b) GO circle plot displaying enrichment analysis for the 7 GO terms with FDR<0.1. Within each selected GO term, blue dot showed a protein underexpressed in colonies “Control Shallow “ compared to control Mesophotic while red dot indicated protein overexpressed. The height of the inner rectangle represents the P value of the GO term. The rectangle is coloured with the blue-red gradient according to the z-score. Z-score = (upregulated – downregulated) / √ (upregulated + downregulated).

(a)

(b)

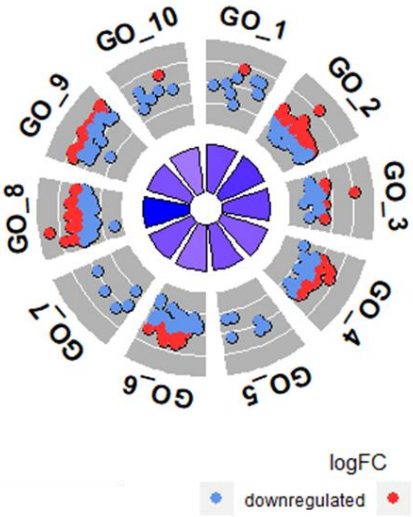

ID	Description
GO_1	cell adhesion mediated by integrin
GO_2	cellular developmental process
GO_3	external encapsulating structure organization
GO_4	negative regulation of developmental process
GO_5	alcohol catabolic process
GO_6	behavior
GO_7	glial cell development
GO_8	response to external stimulus
GO_9	cell development
GO_10	endodermal cell differentiation

ESM8. Gene Ontology (GO) enrichment analysis based on proteins Gene Significance. (a) Hierarchical clustering of enriched biological process gene ontology terms among proteins with the highest gene significance for the comparison Shallow to Mesophotic vs Control Mesophotic. Font size indicates the level of FDR-adjusted statistical significance. Term names are preceded by a fraction indicating the number of individual proteins within each term that are differentially regulated. (b) GO circle plot displaying enrichment analysis for the top 10 GO terms (out of 21 enriched) with the lowest FDR. Within each selected GO term, blue dot showed a protein underexpressed in colonies “Shallow to Mesophotic “ compared to control Mesophotic while red dot indicated protein overexpressed. The outer to inner layers of gray circles indicated the relative fold-change of gene expression (from higher to lower). The height of the inner rectangle represents the P value of the GO term. The rectangle is coloured with the blue-red gradient according to the z-score. Z-score = (upregulated – downregulated) / √ (upregulated + downregulated).

ESM9. Metadata associated with the experiment. It provides details for each sample, including the start and end dates of the experiment, the name of the sampling site along with georeferences in decimal degrees, the treatment they are assigned to and the depths of origin and transplant. Each sample is assigned a unique identifier tag, which can be cross-referenced with deposited raw mass spectrometry data available on the PRIDE partner repository.

Sample	Date beginning	Date end	Sampling site	Latitude	Longitude	Treatment	Origin depth	Transplant depth
BB_10	06/16/2021	11/16/2021	Impérial du Large	43.169861	5.394444	Control Mesophotic	70	70
BB_11	06/16/2021	11/16/2022	Impérial du Large	43.169861	5.394444	Control Mesophotic	70	70
BB_12	06/16/2021	11/16/2023	Impérial du Large	43.169861	5.394444	Control Mesophotic	70	70
BB_13	06/16/2021	11/16/2024	Impérial du Large	43.169861	5.394444	Control Mesophotic	70	70
BB_14	06/16/2021	11/16/2025	Impérial du Large	43.169861	5.394444	Control Mesophotic	70	70
BB_15	06/16/2021	11/16/2026	Impérial du Large	43.169861	5.394444	Control Mesophotic	70	70
BB_9	06/16/2021	11/16/2027	Impérial du Large	43.169861	5.394444	Control Mesophotic	70	70
BT_25	06/16/2021	11/16/2028	Impérial du Large	43.169861	5.394444	Mesophotic to Shallow	70	20
BT_26	06/16/2021	11/16/2029	Impérial du Large	43.169861	5.394444	Mesophotic to Shallow	70	20
BT_27	06/16/2021	11/16/2030	Impérial du Large	43.169861	5.394444	Mesophotic to Shallow	70	20
BT_28	06/16/2021	11/16/2031	Impérial du Large	43.169861	5.394444	Mesophotic to Shallow	70	20
BT_29	06/16/2021	11/16/2032	Impérial du Large	43.169861	5.394444	Mesophotic to Shallow	70	20
BT_30	06/16/2021	11/16/2033	Impérial du Large	43.169861	5.394444	Mesophotic to Shallow	70	20
BT_31	06/16/2021	11/16/2034	Impérial du Large	43.169861	5.394444	Mesophotic to Shallow	70	20
BT_32	06/16/2021	11/16/2035	Impérial du Large	43.169861	5.394444	Mesophotic to Shallow	70	20
TB_17	06/16/2021	11/16/2036	Impérial du Large	43.169861	5.394444	Shallow to Mesophotic	20	70
TB_18	06/16/2021	11/16/2037	Impérial du Large	43.169861	5.394444	Shallow to Mesophotic	20	70
TB_19	06/16/2021	11/16/2038	Impérial du Large	43.169861	5.394444	Shallow to Mesophotic	20	70
TB_20	06/16/2021	11/16/2039	Impérial du Large	43.169861	5.394444	Shallow to Mesophotic	20	70
TB_21	06/16/2021	11/16/2040	Impérial du Large	43.169861	5.394444	Shallow to Mesophotic	20	70
TB_22	06/16/2021	11/16/2041	Impérial du Large	43.169861	5.394444	Shallow to Mesophotic	20	70
TB_23	06/16/2021	11/16/2042	Impérial du Large	43.169861	5.394444	Shallow to Mesophotic	20	70
TB_24	06/16/2021	11/16/2043	Impérial du Large	43.169861	5.394444	Shallow to Mesophotic	20	70
TT_1	06/16/2021	11/16/2044	Impérial du Large	43.169861	5.394444	Control Shallow	20	20
TT_2	06/16/2021	11/16/2045	Impérial du Large	43.169861	5.394444	Control Shallow	20	20
TT_3	06/16/2021	11/16/2046	Impérial du Large	43.169861	5.394444	Control Shallow	20	20
TT_4	06/16/2021	11/16/2047	Impérial du Large	43.169861	5.394444	Control Shallow	20	20
TT_5	06/16/2021	11/16/2048	Impérial du Large	43.169861	5.394444	Control Shallow	20	20
TT_6	06/16/2021	11/16/2049	Impérial du Large	43.169861	5.394444	Control Shallow	20	20
TT_7	06/16/2021	11/16/2050	Impérial du Large	43.169861	5.394444	Control Shallow	20	20